T-2907

The Application Of Ion-Interaction Theory Of Electrolytes To The Solubilities Of Copper And Of Some Alkaline-Earth Sulfates In Brines

by

Daniel C. Melchior

ProQuest LLC.
789 East Eisenhower Parkway
P.O. Box 1346
Ann Arbor, MI 48106 – 1346

T-2907

A thesis submitted to the Faculty and the Board of Trustees of the Colorado School of Mines in partial fulfillment of the requirements for the degree of Doctor of Philosophy in Geochemistry.

Golden, Colorado

Date 11/28/84

Signed: Daniel C. Melchior
Daniel C. Melchior III

Approved: Donald Langmuir
Dr. Donald Langmuir
Thesis Advisor

Golden, Colorado

Date 11/30/84

George Kennedy
Dr. George Kennedy
Chairman Department of
Chemistry/Geochemistry

ABSTRACT

The solubility of well-crystallized tenorite (CuO) was measured in NaCl, Na_2SO_4 and mixed electrolyte solutions between pH 5.8 and 6.5 at various temperatures around 25 and 30°C. A goal was to model Cu^{2+} activity in brines using the ion-interaction solution model (Pitzer, 1979). Tenorite solubilities in 0.009 to 4.1m NaCl, and 0.005 to 0.3m Na_2SO_4 solutions were reversed by lowering the temperature. Ion-interaction calculations showed that only the parameters for $CuCl_2$ and $CuSO_4$ were necessary to accurately model the activity of Cu^{2+} at concentrations below 1×10^{-5} m. The solubility product of tenorite at 25°C based on the modeling is log Ksp = -21.8 ± 0.1 for the reaction: $CuO + H_2O = Cu^{2+} + 2OH^-$. The tenorite solubility experiments in Na_2SO_4 solutions also equilibrated with brochantite [$Cu_4SO_4(OH)_6$]. This leads to log K = -14.0 ± 0.1 for the reaction: $4CuO + SO_4^{2-} + 4H_2O = Cu_4SO_4(OH)_6 + 2OH^-$, and to log Ksp(brochantite) = -73.4 ± 0.1 at 25°C. These solubilities are greater than reported by Barton and Bethke (1960), probably due in large part to particle size effects in their experiments. This study shows that the ion-interaction equations and parameters for major-ion electrolytes may be used to accurately model the activities

of metal cations in brines at the trace concentrations typical of most natural waters.

In a second phase of the study, solubilities of anhydrite ($CaSO_4$), gypsum ($CaSO_4 \cdot 2H_2O$), celestite ($SrSO_4$), barite ($BaSO_4$), and radium sulfate ($RaSO_4$) in waters from the Wolfcamp Formation and granite wash facies, Palo Duro Basin, north Texas were modeled using ion-interaction equations (Pitzer, 1973). Brines with molal ionic strengths ranging from 2.89 to 4.76 and temperatures up to 41°C, and pressures up to 130 bars, were obtained from five horizons in three wells from 967 to 1692 m below the land surface. To assess mineral/saturation relationships, solubility products for each mineral at ground water temperatures and pressures were required for comparison with calculated ion-activity products. Using ion-interaction theory, corrections only in the A_ϕ term were needed to accurately reevaluate published solubility data up to about 100°C. Calculations based on the published data for celestite and gypsum, yielded the following equations where T is absolute:

$$\log Ksp(gypsum) = 68.2401 - 3221.51T^{-1} - 25.0627\log T$$

and

$$\log Ksp(celestite) = 137.555 - 6530.75T^{-1} - 49.419\log T$$

The Ksp values for barite calculated from Blount's (1977) empirical data matched his equation to within 0.02 log units to 175°C; therefore, no new function was determined. The assumption that ΔC_p^o is a constant, independent of temperature for the reaction $Ca^{2+} + BaSO_4(c) = Ba^{2+} + CaSO_4(c)$ (Murray and Cobble, 1980) was used to obtain log Ksp(anhydrite)

$$\log Ksp(anhydrite) = 126.541 - 5038.91T^{-1} - 46.029\log T$$

(Langmuir, 1984). Based on the work of Langmuir and Riese (1984), below about 150°C,

$$\log Ksp(RaSO_4) = 137.98 - 8346.87T^{-1} - 48.5951\log T$$

(Langmuir, 1984) was calculated using a similar approach as for anhydrite.

Modeling results indicated that the five brines are saturated with respect to anhydrite, gypsum, and celestite, and three of the five with barite. The results reflect that the brines have been in contact with overlying evaporite units which probably contain those minerals. However, none of the waters are saturated with respect to $RaSO_4$. Radium concentrations are not controlled by $RaSO_4$ solubility, but may be controlled by the solubility of Ra solid solutions with other sulfate minerals.

TABLE OF CONTENTS

	Page
ABSTRACT	iii
LIST OF FIGURES	ix
LIST OF TABLES	x
ACKNOWLEDGEMENTS	xii
INTRODUCTION	1
ION-INTERACTION APPROACH	4
Theory and General Equations	4
PART I:	
CHEMICAL MODELING OF TENORITE SOLUBILITY IN SALINE WATERS	
PREVIOUS STUDIES OF TENORITE SOLUBILITY	10
EXPERIMENTAL WORK	12
Materials and Reagents	12
Design and Setup	14
EXPERIMENTAL AND MODELING RESULTS	20
NaCl Experiments	23
Na_2SO_4 Experiments	23
EXPERIMENTAL ERRORS	23
Errors in pH Measurement	23
Errors in Ion Interaction Parameters	29
Volumetric, Gravimetric, and Temperature Errors	29
Errors in Copper Analysis	29
Propagation of Errors	30
DISCUSSION OF RESULTS	32
Na_2SO_4 Experiments	32
NaCl Experiments	36

TABLE OF CONTENTS (cont.)

	Page
THE THERMODYNAMIC PROPERTIES OF BROCHANTITE	44
MIXED ELECTROLYTE SYSTEMS	45
CONCLUSIONS	45
RECOMMENDATIONS FOR FUTURE WORK	49
PART II:	
THE THERMODYNAMICS AND GEOCHEMISTRY OF Ca, Sr, Ba, and Ra SULFATES IN SOME DEEP BRINES FROM THE PALO DURO BASIN, TEXAS	
BACKGROUND	51
THE ION INTERACTION APPROACH	54
Temperature and Pressure Corrections to the Ion-Interaction Model	54
THE THERMODYNAMIC DATA BASE	55
Solubility Products of Ca, Sr, Ba and Ra Sulfates	55
Radium Solid Solutions	67
WATER SAMPLING AND CHEMICAL AND ISOTOPIC ANALYSES	69
Sample Collection and Preservation	69
Physical, Chemical and Isotopic Measurements	70
GEOLOGY AND HYDROLOGY OF THE WOLFCAMP FORMATION AND GRANITE WASH FACIES	75
GEOCHEMISTRY OF THE BRINES	76
General Ground Water Geochemistry	76
DISCUSSION MINERAL SATURATION INDICES	78

TABLE OF CONTENTS (cont.)

	Page
CONCLUSIONS	81
REFERENCES CITED	83
APPENDIX A - DETAILED MODELING EQUATIONS	90

LIST OF FIGURES

Figure		Page
1.	Calculated log ion activity product for $CuO + H_2O = Cu^{2+} + 2OH^-$ versus ionic strength of Na_2SO_4 at 25°C.	33
2.	Calculated log ion activity quotient for $4CuO + 4H_2O + SO_4^{2-} = Cu_4SO_4(OH)_6 + 2OH^-$ versus ionic strength of Na_2SO_4 at 25°C.	35
3.	Calculated log ion activity product for $CuO + H_2O = Cu^{2+} + 2OH^-$ versus ionic strength of NaCl at 30°C.	37
4.	Theoretical mean activity coefficient of $Cu(OH)_2$ minus the calculated mean activity coefficient versus molal product of Cu^{2+} and Cl^- ions for the NaCl experiments at 30°C.	41
5.	Calculated log ionic activity quotient for $4CuO + 4H_2O + 2Cl^- = Cu_4Cl_2(OH)_6 + 2OH^-$ versus ionic strength of NaCl at 30°C.	43
6.	Well locations in the Palo Duro Basin, Texas.	77

LIST OF TABLES

Table		Page
1.	Ion interaction virial coefficients at 25°C.	8
2.	Mixing parameters at 25°C that account for higher order electrostatic terms.	9
3.	Thermodynamic properties of selected aqueous species and copper minerals at 25°C and 1bar.	11
4.	Experimental results for the solubility of tenorite in NaCl and Na_2SO_4 solutions.	21
5.	Calculated ion activities in NaCl solutions at equilibrium with tenorite.	24
6.	Calculated ion activities in Na_2SO_4 solutions at equilibrium with tenorite.	26
7.	Difference in theoretical and calculated mean activity coefficients for $Cu(OH)_2$ as a function of the molal product of Cu^{2+} and Cl^- ions.	40
8.	Experimental and calculated activities of species present in four mixed electrolyte systems saturated with respect to tenorite at 30°C.	46
9.	Relative effects on γ_{Ca2+} for a typical brine of the Debye-Hückel Aϕ parameter and of the ion-interaction (I-I) expressions as a function of temperature.	56
10.	Well water temperatures, pressures, and well completion information.	58
11.	The solubility product (-log Ksp) of anhydrite from 25 to 150°C at 1bar.	61
12.	Summary of methods of chemical and isotopic analyses, and their detection limits.	71

LIST OF TABLES (cont.)

Table		Page
13.	Molal concentrations, activity coefficients, and activities, and other chemical properties of the well waters, including pH, molal ionic strength (I) and osmotic coefficients (ϕ).	72
14.	Mineral saturation indices for the five Palo Duro brines, errors in the log Ksp for each mineral given in parenthesis below the name.	80

ACKNOWLEDGMENTS

During the preparation of this dissertation and throughout my educational training I have relied heavily on relatives, friends, and colleagues. I feel that without the love and support of my parents, brother, and wife Christine, that the hurdles would have been much more difficult to clear. My deepest thanks go to them for all they have given me. Thanks must also be given to Jim Ranville for the numerous discussions about brine research and life in general.

Throughout my scientific training I have been fortunate enough to be a student of several fine teachers who have stimulated me to continue on. Much thanks to the Chemistry Department of Southeastern Massachusetts University for the excellent chemistry training I received and the Chemistry and Geology faculties at the Colorado School of Mines.

Much thanks must be given to Dr. Langmuir, my advisor for his insight and help. Collaboration on this and other projects have made me a better scientist and more prepared for the future. I would also like to thank Dr. Pamela Rogers for all her help throughout this project and for the opportunity to more fully appreciate the science and mathematics required in this study. Thanks also to Drs. Closs,

Klusman, Romberger, and Wildeman for serving as committee members.

Lastly I would like to thank the Office of Nuclear Waste Isolation for funding this research under BPMD Contract No. E512-09500, Mr. Ron Kiel and Ms. Carol Kleckner of Geolabs Inc. for their help on the copper analyses, and Mr. Jerry Byrd and Mrs. Dora Rinker of The Earth Technology Corporation for patiently typing this dissertation.

INTRODUCTION

For chemical modeling of aqueous solutions to be useful, the models must be both complete and accurate. In recent years, increased emphasis has been placed on understanding the reaction chemistry of trace constituents in natural water-rock systems. This study examines the mineral/solution equilibria of tenorite (CuO). Tenorite occurs in supergene enrichment zones of copper deposits (Hurlbut and Klein, 1977). It is a sparingly soluble mineral with a pH - dependent solubility. The goal of this study was to chemically model the mineral/solution equilibria of tenorite in solutions of varying composition ranging up to ionic strengths of 4 molal, and to further demonstrate that the model used could be applied to the modeling of many other comparable trace metal/mineral systems.

Aqueous speciation and electrolyte thermodynamics have been examined by numerous authors. Debye and Hückel (c.f. Pitzer and Brewer, 1961) were the first to accurately relate the effective concentration (activity) of an electrolyte to the analytical molality of that electrolyte through an activity coefficient. The activity coefficients calculated by their equation ($\log \gamma \pm = -A(z_+z_-)I^{1/2}$) vary with the stoichiometric or total ionic strength (I) and valence of the ions (z_+ and z_-). A is a constant,

dependent on temperature and pressure. This equation however, is inaccurate in solutions that are not infinitely dilute, because of assumptions inherent in the equation, including that ions do not have finite size and do not interact. Eventually other equations were defined to more accurately account for ion sizes and interactions. Bockris and Reddy (1977) discuss the numerous reasons for the inadequacies of modeling electrolyte interactions using the Debye-Huckel approach.

Most geochemists have assumed an extended Debye-Hückel ion activity coefficient equation, and ion-pair formation to account for the thermodynamic behavior of interacting ions (c.f. Garrels and Thompson, 1962). They have explicitly defined ion pairs and complexes to account for the thermodynamic properties of aqueous ions. This approach can accurately explain the behavior of dilute solutions; however, at high ionic strengths (e.g., above 0.01 to 0.1 m) ion pairing models are generally unable to accurately predict electrolyte activities (c.f. Harvie and Weare, 1980).

Pitzer (1973) developed equations to determine the osmotic and activity coefficients of electrolytes in many dilute and concentrated solutions. His equations were extensions of those proposed by Guggenheim (1935) and Pitzer and Brewer (1961) with modifications for higher

ionic strengths developed by Scatchard (1936). Since 1973, Pitzer and his coworkers (1974a, b) and Pitzer (1975, 1979) have more fully defined the thermodynamic properties of numerous electrolytes using the ion-interaction model. More recently, Harvie and Weare (1980) and Harvie and others (1982) employed ion-interaction equations to predict mineral equilibria involving major ions in saline surface waters.

Part I of this study attempts to model the aqueous solubility of tenorite from pH 5.7 to 6.5 and ionic strengths from 0.009 to 4.10m. The goal is to determine the applicability of ion-interaction theory to the modeling of trace copper activity in brines. If this is achieved, other trace metals of geologic and environmental importance such as Zn, Pb, Co, and Ni could be similarly modeled using comparable ion interaction equations.

Part II considers the solubility of Ca, Sr, Ba, and Ra sulfates, and of trace Ra solid solutions in sulfate minerals in Wolfcamp and granite wash brines from north Texas.

ION-INTERACTION APPROACH

Theory and General Equations

The ion-interaction approach is based on a set of theoretically and empirically derived equations that accurately account for the interactions between aqueous ions and solute water, and the effect that these interactions have on the thermodynamic properties of the ions (Pitzer, 1979). Contained within these equations are ionic strength independent virial coefficients (β^0 and C^ϕ), ionic strength dependent virial coefficients (β^1 and β^2), parameters to account for the effects of mixing unsymmetrical electrolytes (θ_{ij} and ψ_{ijk}), and a modified Debye-Hückel term f^γ. The resulting equation in general form is:

$$\begin{aligned} \ln\gamma_{MX} = {} & |z_m z_x| f^\gamma + (2\nu_M/\nu) \sum_a m_a [B_{Ma} + (\Sigma mz) C_{Ma} \\ & + (\nu_X/\nu_M)\theta_{Xa}] + (2\nu_X/\nu) \sum_c m_c [B_{cX} + (\Sigma mz) C_{cX} \\ & + (\nu_M/\nu_X)\theta_{Mc}] + \sum_c \sum_a m_c m_a \{|z_M z_X| B'_{ca} \\ & + \nu^{-1} [2\nu_M z_M C_{ca} + \nu_M \psi_{Mca} + \nu_X \psi_{caX}]\} \\ & + \tfrac{1}{2} \sum_c \sum_{c'} m_c m_{c'} [(\nu_X/\nu)\psi_{cc'X} \\ & + |z_M z_X| \theta'_{cc'}] + 1/2 \sum_a \sum_{a'} m_a m_{a'} [(\nu_M/\nu) \psi_{Maa'} \\ & + |z_M z_X| \theta'_{aa'}] \end{aligned}$$

where $f^\gamma = -A_\phi \left(\dfrac{I^{1/2}}{1 + 1.2 I^{1/2}} + \dfrac{2}{1.2} \ln(1 + 1.2 I^{1/2}) \right)$,

$A_\phi = 1/3\ A_\gamma$, the Debye-Hückel slope, $I = 1/2 \Sigma_i m_i z_i^2$,

$$B_{MX} = \beta^{O}_{MX} + \frac{2\beta^{1}_{MX}}{\alpha^{2}I}\left[1-(1 + \alpha_1 I^{1/2})\exp(-\alpha_1 I^{1/2})\right]$$

$$+ \frac{2\beta^{2}_{MX}}{\alpha^{2}I}\left[1-(1 + \alpha_2 I^{1/2})\exp(-\alpha_2 I^{1/2})\right]$$

and $C_{MX} = C^{\phi}_{MX} / 2|z_M z_X|^{1/2}$

The terms ν_M and ν_X are the number of ions M (cation) and X (anion) in the neutral salt while ν is the sum of ν_M and ν_X. The electronic charges on the cations and anions are z_M and z_X, respectively. The terms α_1 and α_2 have been empirically derived by Pitzer (1975). For 2-2 electrolytes, $\alpha_1 = 1.4$ and $\alpha_2 = 12.0$. For all other electrolytes $\alpha_1 = 2.0$. B' and θ' are derivatives of those parameters with respect to ionic strength.

The final terms required to accurately model the chemistry of electrolyte mixtures are θ_{ij} and ψ_{ijk}. θ_{ij} accounts for the binary interactions of two unlike ions of the same sign. ψ_{ijk} accounts for the ternary interactions, of two unlike ions of the same sign and an ion of opposite charge. $\theta_{aa'}$ $\theta_{cc'}$ $\psi_{Maa'}$ and $\psi_{cc'x}$ are required when higher order electrostatic terms are used (Pitzer 1975). At the present, there are no terms for quaternary interactions, because it is believed that the statistical and physical likelihood of such interactions is minimal.

The premise of the ion-interaction theory is that electrolyte ions in solution will interact. The importance

of these interactions depends on ionic charges and the statistical probability of ion collisions. The formation of complexes and ion pairs generally need not be defined unless the dissociation constant of the specie is less than about 0.05.

For the most part, the effects of weak ion pairs and complex formation are reflected in the magnitude of the virial coefficients. This is especially critical for 2-2 electrolytes, where the β^2 value is large negative (Pitzer, 1979). A large negative β^2 value indicates that there is a strong attraction between these ions occurring in solution.

Unless the effects of strong complexing are explicitly defined, the stoichiometric ionic strength ($I = \frac{1}{2}\sum_i m_i z_i^2$) is used in all calculations. All of the parameters except for f^γ, α_1, and α_2 have been determined from least square fitting of isopiestic, EMF, and solubility data in like-ion solutions. In some systems, it is possible to determine some of the parameters from unlike-ion solutions if other parameters are known from previous work (c.f. Downes and Pitzer, 1976).

Of the three methods used in parameter determination, solubility experiments are the least preferred, and pH dependent solubility experiments are the least preferred of solubility experiments (Harvie, 1981).

The algorithm used in this study also contains temperature derivatives of the parameters and a function to determine the correct A_ϕ value for the temperature in question (Pitzer 1979). The importance of temperature functions is discussed by Melchior and others (1984). In that study, a function was fit to values of A_ϕ versus temperature given by Pitzer (1979). The function is $A_\phi = 3.8 \times 10^{-6} t^2 + 4.724 \times 10^{-4} t + 0.3769$ where t is in Celsius.

Table 1 and 2 list the ion-interaction parameters and thermodynamic data used in this study. The model used in this study accounts for the purely electrostatic effects of mixing unsymmetrical electrolytes as discussed by Pitzer (1975). Parameters not listed may be found in Pitzer (1979). Discussion of parameter standard deviations is given by Pitzer (1979). However, the errors related to the original experimental data are not quantified.

The ion-interaction equations appropriate to the tenorite solubility experiments are presented in Appendix A.

Table 1. Ion interaction virial coefficients at 25°C, from Pitzer (1979) and Downes and Pitzer (1976).

Electrolyte	β_0	β_1	β_2	C^ϕ
NaCl	0.07650	0.26640	0.000	0.00127
Na_2SO_4	0.01958	1.11300	0.000	0.00570
NaOH	0.08640	0.25300	0.000	0.00440
KCl	0.04835	0.21220	0.000	-0.00084
K_2SO_4	0.04995	0.77925	0.000	0.00000
KOH	0.12980	0.32000	0.000	0.00410
$CuCl_2$	0.29662	1.39125	0.000	-0.03602
$CuSO_4$	0.23400	2.52700	-48.330	0.00440

Table 2. Mixing parameters that account for higher order electrostatic terms at 25°C, from Downes and Pitzer (1976).

Cations	Anions	θ_{ij}	ψ_{ijk}
Na^+ Cu^{2+}	Cl^-	0.077	-0.026
	SO_4^{2-}		-0.049
Anions	**Cation**	θ_{ij}	ψ_{ijk}
Cl^- SO_4^{2-}	Na^+	0.030	0.000
	K^+		-0.005
	Mg^{2+}		-0.020
	Cu^{2+}		0.031

PREVIOUS STUDIES OF TENORITE SOLUBILITY

The solubility of tenorite has been examined in several other studies. Feitknecht and Schindler (1963) measured the solubility of CuO as a function of its relative "activity" or degree of crystallinity. In their study they titrated alkaline solutions into cupric solutions to precipitate $Cu(OH)_2$. They noticed that the relative degree of crystallinity increased within a few days. They also observed that when precipitates were heated the degree of crystallinity increased. Feitknecht and Schindler found that the level of crystallinity can affect the solubility product of CuO at 298K by at least ± 0.8 log units. Schindler (1968) further showed that the solubility of all metal oxides is dependent upon molar surface area.

The log solubility product (K) for the reaction, $CuO + H_2O = Cu^{2+} + 2OH^-$ given by Barton and Bethke (1960) is -19.7 ± 0.4. On the other hand, using free energies in Table 3, including ΔG_f° (CuO) from Robie and others (1978), the calculated log K = -20.6. This latter value is presumably for a well crystallized solid. Whereas, the value given by Barton and Bethke (1960) is for poorly crystallized material (c.f. Schindler, 1968).

McDowell and Johnston (1936) studied the solubility of tenorite in alkaline solutions. Equilibrium was approached from undersaturation and supersaturation using temperature

Table 3. Thermodynamic properties of selected aqueous species and copper minerals at 25°C and 1 bar.

Mineral or aqueous species	ΔH°_f (kcal/mol)	ΔG°_f (kcal/mol)	S° (cal/deg mol)	Reference
Cu^{2+}	15.7	15.68	-23.21	CODATA (1977)
CuO(c) (Tenorite)	-37.60 / -39.2*	-30.97 / -32.6*	10.19	Robie and others (1978)
$Cu_4Cl_2(OH)_6$(c) (Atacamite)	-390.77	-320.06	88.5	Duby (1977)
$Cu_4SO_4(OH)_6$(c) (Brochantite)	(-520.9)/(-566.34)*	-434.42/-441.0*	(87.9)	Duby (1977) S° estimated by Langmuir (1983)
H_2O	-68.315	-56.687	16.71	CODATA (1976)
OH^-	-54.977	-37.604	-2.560	CODATA (1976)
Cl^-	-39.933	-31.379	13.56	CODATA (1976)
SO_4^{2-}	-217.40	-177.95	4.50	CODATA (1977)
	$K_w = 10^{-14.00}$ at 25°C			Olofsson and Olofsson (1981)
	$K_w = 10^{-13.84}$ at 30°C			

* Calculated from solubility experiments in this study.

as the reversal mechanism. They agitated their experimental vessels at both 25° and 45°C for four days and then transferred all experiments to 25°C baths for 14-50 days. Their results indicate reversal was complete within 14 days and that copper concentrations in solution did not change up to the 50 day maximum. Majima and others (1980) also examined the dissolution of tenorite. Their study showed that the rate of solution was independent of the solution agitation rate.

Several studies have compared the stability of tenorite to that of other cupric minerals as a function of solution composition. Schindler (1968) has shown that the P_{CO_2} in equilibrium with water must equal 10^{-1} before tenorite is unstable with respect to malachite. Schindler (1968) also shows that cupric ion is the stable form of aqueous Cu(II) up to pH 8 in CO_2 saturated water. Barton and Bethke (1960) have measured and computed the equilibrium relationships between tenorite (CuO) and both brochantite ($Cu_4SO_4(OH)_6$), and atacamite ($Cu_4Cl_2(OH)_6$).

EXPERIMENTAL WORK

Materials and Reagents

All of the compounds used in the experimental work were ACS Reagent Grade or better. Non-copper reagents were checked for copper content before experimentation by

preparing blank solutions with doubly-deionized water, and were found to contain less than 10 ppb copper.

Analytical grade tenorite wire (prepared from 99.99% Cu) from Fisher Scientific Company was used in all experiments. The tenorite had been made by oxidizing the copper wire in a furnace. The CuO, in wire form was boiled in 0.05% HCl solution for two weeks to remove fine particles and other copper minerals that might be present, and to create a clean surface. Once cleaned, the wire was placed in a 110°C oven overnight to evaporate any remaining water.

Cleaned tenorite was stored in a dessicator with fresh dessicant until used. X-ray diffraction analysis of a pulverized sample showed no evidence of line broadening, which indicates that few fine particles (<10Å) existed. The pattern showed that both CuO and Cu_2O were present and their relative amounts varied within individual wires. The Cu_2O should not have affected the solubility experiments because CuO is the stable oxide phase in air saturated water and if it was present after all the CuO dissolved it would have oxidized. At the end of all experiments some wire remained that contained both CuO and Cu_2O indicating there was still a solid CuO phase with which to equilibrate.

All glassware and pipets were calibrated and found to be within the guidelines for Class A volumetric ware.

Epindorf pipets were accurate to ± 1 percent. Before use, all Epindorf pipet tips were soaked in 1:1 HNO_3 solution for two weeks followed by five rinses with doubly deionized water and air drying.

The analytical balance used was calibrated and found accurate to ± 0.0001g. The thermometers were accurate to ± 0.1°C over a temperature range of 0 to 100°C based on the manufacturer's calibration against NBS calibrated thermometers.

Design and Setup

Cells made of Pyrex were fabricated from 1000 ml beakers by bending down the edge to form a lip, which was ground flat. Prior to use, all cells were soaked with 1:1 HNO_3 solution for two days and rinsed eight times with doubly deionized water. Silicone stopcock grease was spread on the cell lip and a lid made of plexiglas with several holes for each cell was placed on top, forming a seal against the cell lip. Gum rubber stoppers were used to fill all the holes. A floating stirbar was placed in each cell to agitate the solution during the experiment. Approximately 0.1g of CuO was placed in each cell. Freshly deionized water with a pH of between 6.5 and 7.5 was pipetted into each cell after it was purged with oxygen or CO_2-free air. The CO_2-free air was obtained by bubbling air through two $Ca(OH)_2$-saturated solutions and three

vessels of water. Once this was complete, measured amounts of NaCl were placed in each cell. Duplicate cells were prepared so that under and supersaturated runs could be made. Each cell was placed in a temperature controlled water bath with magnetic stirrers underneath and maintained at 25.0 ± 0.5°C and 35.0 ± 0.5°C.

Prior to completing the experiments, the pH of several cells was taken. All pH's were below 5.5 with one below 5.0. This indicated that problems existed with the experimental design. In addition, bacterial growth in two cells was noticed, and the CuO wire was being ground into a fine powder by movement of the floating stirbar. For these reasons, a controlled experiment was set up. A single pyrex cell was prepared as earlier discussed. In addition, another was rinsed with 1.0m NaCl for three rinses followed by three rinses with doubly deionized water. This was to determine if exchange of Na^+ with protons was occurring on glass vessel walls and if rinsing with NaCl could prevent it. Both cells were purged of CO_2, and a 1.0m NaCl solution of pH between 6.5 to 7.0 was added. Both cells sat for several days and the pH's were taken. Final pH's were below 5.0. This indicated that acid was either being released through cation exchange or from surface cavities. Because borosilicate glass and plastics such as plexiglass are known to contain relatively high amounts of base metals

including copper (Robertson, 1968) acid washing was necessary, yet could not be done due to the proton release problem. The continual evolution of protons to the system would preclude that system ever reaching equilibrium within a reasonable length of time. Thus, a better design was required.

Due to the problems associated with glass cells, Nalgene bottles composed of linear polyethylene were chosen. Moody and Lindstrom (1977) investigated the use of linear polyethylene bottles for preservation of water samples and found that the bottles contained less than 2 ppb leachable copper using 1:1 HNO_3. Subramanian and others (1978) showed that the loss of copper from unpreserved samples was minimal and was complete after one day. Therefore the reaction cell had quickly equilibrated with the solutions.

Prior to conducting any solubility experiments, a 125 ml Nalgene bottle was soaked with 1:1 HNO_3 solution and rinsed eight times with doubly deionized water. The bottle was then filled with 0.5m NaCl which had an initial pH of between 6.5 and 7.0. The pH was measured after a week. The results indicated that again, acid washing of a reaction vessel is unacceptable since the pH was 5.4 and proton release was evident.

The preferred preparation method was determined to be a washing of each bottle with a dilute ALCONOX soap/doubly deionized water solution followed by ten rinsings with doubly-deionized water. Each bottle was turned upside down to dry. The pH of deionized air saturated water following this treatment was 5.7.

Once it was decided that 125 ml Nalgene bottles could be used as reaction vessels, the experiments were begun. In each bottle, the appropriate mass of solute (NaCl or Na_2SO_4) and approximately 0.05 to 0.1g of CuO wire were placed. The air in each bottle was purged with CO_2-free air or oxygen for 10 minutes even though Schindler (1968) has shown that tenorite is the stable phase at atmospheric CO_2 pressures. Subsequent to this, freshly deionized water was pipetted into each bottle and the bottle capped. Each bottle was placed in the appropriate shaking temperature control bath.

Based on work by previous authors as discussed earlier, it was decided that all reactions would be reversed through changes in temperature as described in McDowell and Johnston (1936). Barton and Bethke (1960) showed that tenorite solubility obeys a van't Hoff behavior as a function of temperature. Assuming dissolution of CuO to Cu^{2+} and OH^-, with ΔH_f° (CuO) = -37.60 kcal/mol is 11.66 kcal/mol. Assuming a solubility product of 10^{-21} and

constant pH, a temperature increase of 5°C leads to an approximately 40 percent increase in copper concentration. Thus, it is possible to determine if equilibrium has been reached by determining copper concentrations in the high and low temperature runs.

The experiments with sodium sulfate and tenorite were maintained at 25.0 and 30.0 ± 0.5°C and run for two weeks. After two weeks, all of the reaction cells in the 30°C bath were transferred to the 25°C bath for three additional weeks. Subsequent to this, agitation was stopped for one hour during which time pH buffers were placed in the bath to allow them to reach thermal equilibrium with the cells. Following thermal equilibration, the pH electrode and meter were doubly calibrated with pH 4.01 ± 0.02 (potassium hydrogen phthalate) and 6.86 ± 0.02 (potassium hydrogen phosphate buffers (Bates 1964). The electrode slope agreed with Nernstian behavior each time measurements were taken to within ± 0.2 mV at 25°C. Once calibrated, the reaction cells were removed from the temperature controlled bath and their pH measured. The electrode was allowed to stabilize until the value on the meter remained constant in the second decimal place for three minutes. This process usually took five to ten minutes for each sample. Once all of the reaction cell pH's were measured, two cell pH's were

remeasured. The pH's of the sodium sulfate experiments were reproducible to ± 0.05 pH units.

The solution in each cell was then filtered and acidified for analysis. Filtration was with 0.2μ nucleopore polycarbonate filters that had been prepared by acid washing for two weeks, rinsing with doubly deionized water and drying. The membrane supports used were also made of polycarbonate, as Truitt and Weber (1979) have shown that cellulose membranes and glass supports remove metals from solutions. Each sample was filtered using standard rinsing techniques such as rinsing the supports, pipets, and bottles with an aliquot of the filtered solution prior to filtration and preservation. In addition, standards were exposed to the same filtration, transfer, and rinsing procedures. Subsequent to filtration, aliquots were pipetted into acid-rinsed Nalgene bottles using plastic pipets and acidified to a pH 2 to preserve the sample, and finally capped (Subramanian and others, 1978). All samples were analyzed by flame atomic absorption spectroscopy by an independent laboratory using a standard additions method.

Analogous experiments were conducted in sodium chloride solutions and in some synthetic brines. Experimental procedures were identical for the NaCl experiments, except that initial temperatures of 30 and 36°C were used, with the 36°C set of experiments reversed after two weeks

to 30°C. The synthetic brines were maintained at 30°C throughout the run.

During pH measurement, slow pH drift was encountered. Consequently, measurements took from ten to twenty minutes and pH's were reproducible to ± 0.05 units at ionic strengths less than 1m, and ± 0.1 units above one molal. The reproducibility was checked in several cells by remeasuring the pH after all cells had been measured once.

A continuous leakage of carbon dioxide from the air probably occurred through the portion of the reaction cell and cap not submerged in the bath. At this altitude (1640 m), water saturated with air has a pH of 5.7. The most dilute NaCl and Na_2SO_4 solutions had pH's of 5.7 indicating that atmospheric carbon dioxide equilibrated with the system.

EXPERIMENTAL AND MODELING RESULTS

Analyses of dissolved copper, measured pH, and electrolyte molalities at equilibrium, for all the experiments are presented in Table 4. The analyzed copper standards showed that the accuracy and precision of the measurements was ± 5-10 percent at all ionic strengths. Measured pH's were corrected for liquid junction potentials using the Henderson-Planck equation (Bates, 1964). Further discussion of this correction is given within the experimental

Table 4. Experimental results for the solubility of tenorite in NaCl and Na_2SO_4 solutions. Runs approached from undersaturation are denoted by L or SL, or from supersaturation by H or SH.

Table 4a. NaCl experiments. Final run temperature was 30°C.

Run	mNa^+	$(mCu^{2+}) \times 10^6$	mCl^-	Measured pH	Thermodynamic pH
1L	0.0094	4.60	0.0094	5.69	5.74
1H	0.0095	5.89	0.0095	5.71	5.76
2L	0.0456	6.76	0.0456	5.82	5.86
2H	0.0457	5.47	0.0457	5.87	5.91
3L	0.0911	6.18	0.0911	5.85	5.88
3H	0.0912	7.77	0.0912	5.88	5.91
4L	0.3011	6.36	0.3011	6.02	6.03
4H	0.3011	5.06	0.3011	6.07	6.08
5L	0.6020	5.24	0.6020	6.08	6.07
5H	0.6020	5.38	0.6020	6.13	6.12
6L	0.9121	5.41	0.9121	6.30	6.28
6H	0.9122	4.68	0.9122	6.24	6.22
7L	1.8245	5.53	1.8245	6.25	6.21
7H	1.8245	4.63	1.8245	6.25	6.21
8L	2.2806	5.44	2.2806	6.32	6.27
8H	2.2806	5.75	2.2806	6.28	6.23
9L	2.7366	5.66	2.7366	6.44	6.38
9H	2.7367	5.66	2.7367	6.52	6.46
10L	3.1926	9.13	3.1926	6.09	6.03
10H	3.1927	9.13	3.1927	6.10	6.04
11L	4.1048	13.21	4.1048	6.26	6.19
11H	4.1048	13.21	4.1048	6.36	6.29

Table 4b. Na_2SO_4 experiments. Final run temperature was 25°C.

Run	mNa^+	(mCu^{2+}) $x10^6$	mSO_4^{2-}	Measured pH	Thermo-dynamic pH
1SL	0.0100	6.31	0.0050	5.74	5.79
1SL	0.0101	5.83	0.0051	5.67	5.72
2SL	0.0201	5.52	0.0100	5.86	5.91
2SH	0.0200	5.84	0.0100	5.90	5.95
3SL	0.1004	5.52	0.0502	5.96	6.00
3SH	0.1005	5.84	0.0502	5.90	5.94
4SL	0.2007	4.90	0.1004	6.01	6.04
4SH	0.2007	5.21	0.1004	5.99	6.03
5SL	0.3512	5.53	0.1756	6.11	6.14
5SH	0.3512	5.22	0.1756	6.03	6.06
6SL	0.5017	3.96	0.2508	6.01	6.04
6SH	0.5017	5.22	0.2508	6.03	6.06
7SL	0.6020	4.60	0.3010	6.09	6.12
7SH	0.6020	4.60	0.3010	6.01	6.04

error-pH measurement section below. Corrected pH's are listed in Table 4.

NaCl Experiments

Results of the tenorite solubility runs in NaCl solutions were modeled with the ion interaction algorithm using the equations given in Appendix A. Results were modeled with and without the cupric chloride virial coefficients and mixing parameters (see Table 5). The purpose of this comparison was to determine the effect of the published parameters on the activity of copper derived from the dissolution of a second copper phase (i.e., CuO).

Na_2SO_4 Experiments

Results of the CuO solubility measurements in Na_2SO_4 solutions were modeled with the ion interaction algorithm for the equations presented in Appendix A. Again, and for the same reason, modeling was performed with and without the cupric sulfate virial coefficients and mixing parameters. Ion activities computed with both assumptions are presented in Table 6.

EXPERIMENTAL ERRORS

Errors in pH Measurement

All pH measurements were taken using the procedures outlined by Bates (1964) and Midgley and Torrance (1978) with exception that all solutions were gently swirled and

Table 5a. Calculated ion and water activities in NaCl solutions at equilibrium with tenorite. The modeled results were obtained with (column a) and without (column b) the $CuCl_2$ parameters. Na^+, Cl^-, OH^-, and H_2O activities were identical using either approach.

Run	Na^+,Cl^-	$(Cu^{2+})x10^6$ (a)	$(Cu^{2+})x10^6$ (b)	$(OH^-)x10^8$	H_2O
1L	0.0085	3.03	2.94	0.752	1.000
1H	0.0086	3.88	3.76	0.834	1.000
2L	0.0376	3.05	2.68	1.05	0.998
2H	0.0377	2.46	2.16	1.18	0.998
3L	0.0712	2.24	1.76	1.10	0.997
3H	0.0712	2.81	2.21	1.17	0.997
4L	0.212	1.54	0.812	1.54	0.990
4H	0.212	1.22	0.646	1.73	0.990
5L	0.402	1.03	0.354	1.67	0.980
5H	0.402	1.06	0.363	1.87	0.980
6L	0.597	0.975	0.233	2.66	0.970
6H	0.597	0.843	0.202	2.33	0.970
7L	1.200	0.941	0.100	2.20	0.938
7H	1.200	0.789	0.0841	2.20	0.938
8L	1.540	0.939	0.0729	2.48	0.921
8H	1.540	0.991	0.0770	2.27	0.921
9L	1.900	0.996	0.0587	3.13	0.904
9H	1.900	0.996	0.0587	3.77	0.904
10L	2.300	1.64	0.0758	1.37	0.886
10H	2.300	1.64	0.0758	1.41	0.886
11L	3.220	2.44	0.0758	1.91	0.847
11H	3.220	2.44	0.0758	2.41	0.847

Table 5b. Calculated ionic activity quotients: for the dissolution of tenorite via the reaction $CuO + H_2O = Cu^{2+} + 2OH^-$ with (column a) and without (column b) the $CuCl_2$ parameters; and in column c for the formation of atacamite via the reaction $4CuO + 2Cl^- + 4H_2O = Cu_4Cl_2(OH)_6 + 2OH^-$ using all parameters. The error attributed to the log of the quotients is ± 0.1 units for runs 1 through 6 and ± 0.2 units for later runs.

Run	$\log \frac{(Cu^{2+})(OH^-)^2}{(H_2O)}$ (a)	$\log \frac{(Cu^{2+})(OH^-)^2}{(H_2O)}$ (b)	$\log \frac{(OH^-)}{(Cl^-)(H_2O)^2}$ (c)
1L	-21.7	-21.8	-6.0
1H	-21.6	-21.6	-6.0
2L	-21.5	-21.5	-6.6
2H	-21.5	-21.5	-6.5
3L	-21.6	-21.7	-6.8
3H	-21.4	-21.5	-6.8
4L	-21.4	-21.7	-7.1
4H	-21.4	-21.7	-7.1
5L	-21.5	-22.0	-7.4
5H	-21.4	-21.9	-7.3
6L	-21.2	-21.8	-7.4
6H	-21.3	-22.0	-7.4
7L	-21.3	-22.3	-7.7
7H	-21.4	-22.4	-7.7
8L	-21.2	-22.4	-7.8
8H	-21.3	-22.4	-7.8
9L	-21.0	-22.2	-7.8
9H	-20.9	-22.1	-7.7
10L	-21.5	-22.9	-8.2
10H	-21.5	-22.8	-8.2
11L	-21.1	-22.6	-8.2
11H	-20.9	-22.4	-8.1

Table 6a. Calculated ion and water activities in Na_2SO_4 solutions at equilibrium with tenorite. The modeled Cu^{2+} results were obtained with (column a) and without (column b) the $CuSO_4$ parameters. Na^+, SO_4^{2-}, OH^- activities were identical using either approach.

Run	$(Na^+)x10^2$	$(Cu^{2+})x10^6$ (a)	$(Cu^{2+})x10^6$ (b)	$(SO_4^{2-})x10^2$	$(OH^-)x10^8$	H_2O
1SL	0.887	3.10	3.66	0.302	0.617	1.000
1SH	0.897	2.85	3.38	0.304	0.525	1.000
2SL	1.71	2.09	2.61	0.506	0.813	1.000
2SH	1.70	2.21	2.76	0.505	0.891	1.000
3SL	7.52	0.998	1.23	1.38	1.00	0.998
3SH	7.53	1.06	1.30	1.38	0.871	0.998
4SL	14.1	0.633	0.670	1.91	1.10	0.996
4SH	14.1	0.674	0.713	1.91	1.07	0.996
5SL	23.1	0.546	0.469	2.37	1.38	0.993
5SH	23.1	0.514	0.442	2.37	1.15	0.993
6SL	31.7	0.329	0.237	2.65	1.10	0.990
6SH	31.7	0.435	0.312	2.65	1.15	0.990
7SL	37.1	0.351	0.227	2.78	1.32	0.988
7SH	37.1	0.351	0.227	2.78	1.10	0.988

Table 6b. Calculated ionic activity quotients: for the dissolution of tenorite via the reaction $CuO + H_2O = Cu^{2+} + 2OH^-$ with (column a) and without (column b) the $CuSO_4$ parameters; and in column (c) for the formation of brochantite via the reaction $4CuO + SO_4^{2-} + 4H_2O = Cu_4SO_4(OH)_6 + 2OH^-$. Brochantite quotients are identical when computed with or without $CuSO_4$ parameters. Error attributed to the log of the quotients are all ± 0.1 units.

Run	$\log \frac{(Cu^{2+})(OH^-)^2}{(H_2O)}$ (a)	$\log \frac{(Cu^{2+})(OH^-)^2}{(H_2O)}$ (b)	$\log \frac{(OH^-)}{(SO_4^{2-})(H_2O)^4}$ (c)
1SL	-21.9	-21.9	-13.9
1SH	-22.1	-22.0	-14.0
2SL	-21.9	-21.8	-13.9
2SH	-21.8	-21.7	-13.8
3SL	-22.0	-21.9	-14.1
3SH	-22.1	-22.0	-14.3
4SL	-22.1	-22.1	-14.2
4SH	-22.1	-22.1	-14.2
5SL	-22.0	-22.1	-14.1
5SH	-22.2	-22.2	-14.2
6SL	-22.4	-22.5	-14.3
6SH	-22.2	-22.4	-14.3
7SL	-22.2	-22.4	-14.2
7SH	-22.4	-22.5	-14.3

not stirred, to minimize flowing potentials. In high ionic strength solutions, the measured pH differs from the thermodynamic solution pH because of liquid junction potential effects (Bates, 1964). The error in pH measurement due to the liquid junction potential (E_j) may be estimated using the Henderson-Planck equation (Bates, 1964). This equation relates the mobilities and concentrations of ions in the solution to the same properties of the KCl solution in the outer body of the reference electrode. The result is the estimated potential difference between the two solutions. This E_j correction is converted to pH units by dividing by the Nernstian slope, and then added to the measured pH. The result is an estimate of the thermodynamic pH. Ionic mobilities used in these calculations were from Robinson and Stokes (1959).

There is no published literature that addresses the errors involved with pH measurements in poorly buffered, saline waters. The reproducibility of the measurements has been discussed earlier. It is clear that the accuracy of pH measurements is difficult to assess because of long drift times. Bates (1964) has shown that for a high sodium glass electrode such as the Orion 91-02 used in this study there is no electrode selectivity correction needed up to 1 molal Na^+ over a pH range of 5.7 to 6.5. Bates does not consider corrections for solutions greater than one molal.

Errors in Ion Interaction Parameters

Uncertainties in the ion interaction parameters are unknown. No previous authors have addressed this problem. To estimate uncertainties, a complete error analysis of the original data used by Pitzer (1973) and subsequent authors is needed. However, because all the parameters are interrelated, the task would be monumental. Hence, such parameters are assumed accurate by this and other authors. The only check on the accuracy of the parameters is through the successful application of the ion interaction model to other systems.

Volumetric, Gravimetric, and Temperature Errors

Based on calibrations of the analytical balance and transfer pipets, errors do not exceed 0.01 percent in calculations involving masses and volumes.

The temperature measurements are accurate to $\pm$ 0.1°C, whereas temperature control was maintained to within $\pm$ 0.5°C. By using a van't Hoff approximation for CuO solubility, an error in temperature of $\pm$ 0.5K would yield an error in dissolved copper of 7.9 percent.

Errors in Copper Analysis

Chemical analyses of standard solutions with copper concentrations between 30 ppb and 1 ppm indicated that high ionic strengths did not affect analytical results, using

the standard addition technique. Errors in the standards varied from ± 5 to 10 percent independent of ionic strength. Maximum errors of ± 10 percent in the copper analyses using the standard additions method are probable.

Propagation of Errors

To decide if the experimental data in this study require ion interaction parameters in addition to those published to explain deviations in electrolyte activities it is necessary to determine errors in the modeled ion activity products. Such errors involve the operations of multiplication and division (Skoog and West, 1974). The calculated error in cupric ion activity is primarily a function of uncertainties in Cu(II) analysis and temperature. Errors in the activity of aqueous hydroxide are a function of the pH error. The reproducibility of the pH measurements was assumed equal to their accuracy. The error in the calculated activity of water depends on the accuracy of the osmotic pressure (ϕ) measurements obtained in mixed electrolyte solutions. The uncertainty in ϕ for different individual electrolytes at the same ionic strengths do not exceed ± 0.1 percent at 25°C (c.f. Latimer, 1952: Harned and Owen, 1958: and Robinson and Stokes, 1959).

Following is an example calculation of the relative percent error of a solubility product (K) of CuO measured in a 0.5m NaCl solution.

$$\% \text{ error}(K) = ((\% \text{ error in Cu analysis})^2 + (\% \text{ error in Cu due to temperature bath fluctuation})^2 + 2(\% \text{ error in } OH^- \text{ based on pH reproducibility})^2)^{1/2}$$

$$= ((10)^2 + (7.9)^2 + 2(10)^2)^{1/2}$$

$$= 19$$

for the $(Cu^{2+})(OH^-)^2/(H_2O)$ ion activity product. A 19 percent error is equivalent to an error of 0.1 log unit in the calculated ion activity product, the same as the error attributed to the pH measurement. The error in the ion activity product resulting from the uncertainty in the pH is greater in more saline waters where long drift times make pH measurement very subjective. Errors calculated using this conservative method are given with the calculated ion activity products in Tables 5 and 6. Errors attributed to the experiments in very saline systems (>1m) may be greater than listed, but are not quantifiable.

DISCUSSION OF RESULTS

The calculated ion activity products for dissolution of tenorite in NaCl and Na_2SO_4 solutions are presented as a function of major electrolyte molalities in Figures 1, 2, and 3.

Na_2SO_4 Experiments

A linear regression fit line through the modeled data using the equations in Meyer (1975) and incorporating the uncertainties assigned to each value considering the $CuSO_4$ virial coefficients yields a log solubility product for tenorite at infinite dilution of -21.9 ± 0.10 as shown in Figure 1. The value of -21.9 is within the error limit for the log solubility product of tenorite of ± 1.5 units as reported by Barton and Bethke (1960). Barton and Bethke's (1960), tenorite solubility experiments were not reversed and probably involved a variety of particle sizes, such as found by Schindler (1965) in his experiments. Based on Schindler's (1968) equation and the thermodynamic solubility product determined here, $\log K = -21.9 + (8.0 \times 10^{-5})s$ where s is the molar surface area. Barton and Bethke's (1960) log Ksp of -19.7 for tenorite suggests a CuO molar surface area of $27{,}500 \pm 7500 m^2$. This area is much larger than likely based on Schindler's study.

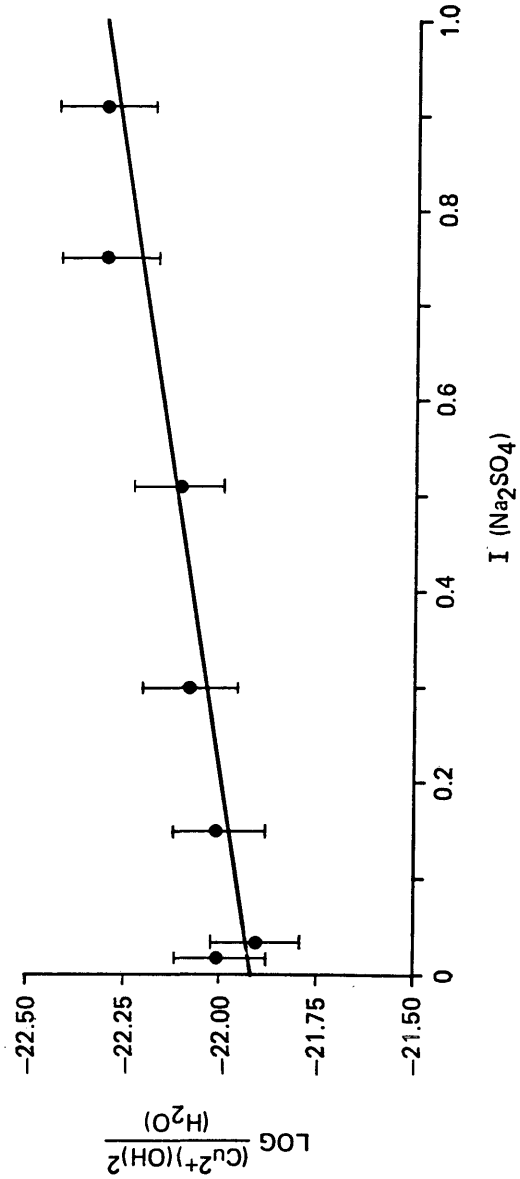

Figure 1. Calculated log ion activity product for $CuO + H_2O = Cu^{2+} + 2OH^-$ versus ionic strength of Na_2SO_4 at 25° C. Data points are averages of undersaturated and supersaturated runs. Error bars are discussed in the text. A regression fit (solid line) of the data yields an intercept of -21.9, a slope of -0.42 and $r^2 = 0.66$.

Feitknecht and Schindler (1963) have shown that $Cu(OH)_2$ will precipitate if cupric ion is titrated with alkali solutions and later recrystallize to form CuO. The Ksp for tenorite given by Barton and Bethke (1960) may in fact reflect the presence of minor poorly crystalline $Cu(OH)_2$. The question remains if CuO was present at the end of Barton and Bethke's (1960) experiments or if the $Cu(OH)_2$ converted prior to the X-ray diffraction study. The free energy of reaction obtained by using the solubility product of $10^{-21.9}$ determined in the Na_2SO_4 experiments is 29.9 ± 0.1 kcal/mol. The enthalpy of reaction is 14.0 ± 0.1 kcal/Mol. The free energy and enthalpy of formation of tenorite will be calculated later after the 30° NaCl measurements are analyzed and the results can be averaged.

The activity of sulfate was computed for experiments thought to have equilibrated with both tenorite and brochantite via the reaction $4CuO + SO_4^{2-} + 4H_2O = Cu_4SO_4(OH)_6 + 2OH^-$. Figure 2 shows a plot of the log ion activity quotient for $(OH^-)^2/(SO_4^{2-})(H_2O)^4$ versus ionic strength considering the $CuSO_4$ virial coefficients the intercept of the linear regression line is -14.0 ± 0.1. The uncertainty is the square root of the sum of the squares of the individual errors. These results are within the uncertainty in Barton and Bethke (1960) value of -14.2 ± 1.5. Based on

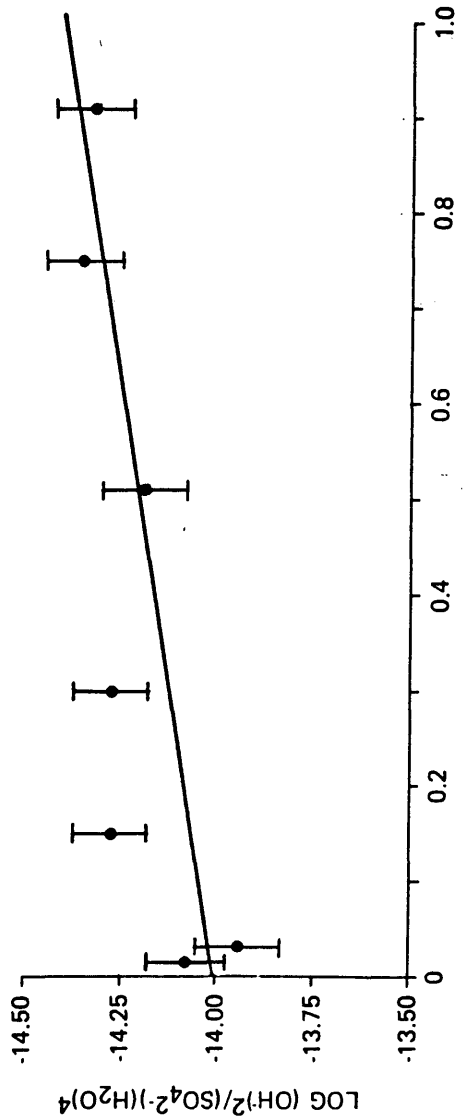

Figure 2. Calculated log ion activity quotient for $4CuO + 4H_2O + SO_4^{2-} = Cu_4SO_4(OH)_6 + 2OH^-$ versus molal stoichiometric ionic strength of Na_2SO_4 at 25° C. Data points are averages of undersaturated and supersaturated runs. Error bars are discussed in the text. A regression fit (solid line) of the data yields an intercept of -14.0, a slope of -0.30 and r^2 = 0.53.

the relative constancy of the ion activity product for the tenorite-brochantite reaction, it is probable that all of the sulfate experiments equilibrated with phases. To substantiate this hypothesis X-ray diffraction patterns were obtained for the starting solid substrate and the residue of the solution in run 4SH. Brochantite was not identified in either the solid or dried residue indicating it's absence at a greater than one percent level, the approximate sensitivity of the method.

A comparison of the calculated ion activity products with and without the $CuSO_4$ virial coefficients and parameters in Table 6 shows that the difference never exceeds 0.2 log units up to 0.3 molal sulfate concentrations. For most natural systems, the aqueous sulfate content will not exceed the 0.3 molal maximum used in this study as gypsum, anhydrite, and/or other sulfate minerals will control sulfate activities, and thus the relative importance of the $CuSO_4$ parameters on Cu(II) activity is negligible for most natural waters.

NaCl Experiments

Data for the solubility of tenorite in NaCl solutions at 30°C was modeled with the ion interaction approach. Results are plotted in Figure 3 as the log of the ion

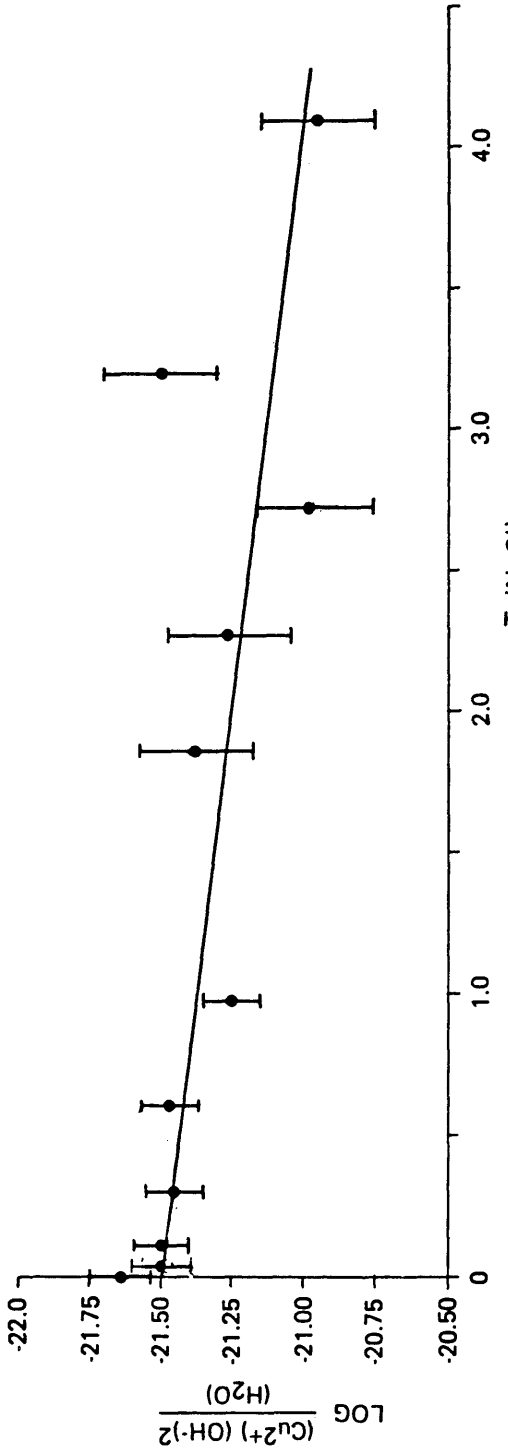

Figure 3. Calculated log ion activity product for $CuO + H_2O = Cu^{2+} + 2OH^-$ versus I (NaCl) at 30° C. Data points are averages of undersaturated and supersaturated runs. Error bars are discussed in the text. A regression fit (solid line) of the data yields an intercept of -21.5, a slope of 0.12 and $r^2 = 0.46$.

activity quotient for the reaction $CuO + H_2O = Cu^{2+} + 2OH^-$ versus stoichiometric ionic strength. A regression line, as discussed earlier, considering $CuCl_2$ virial coefficients indicates that the solubility product of tenorite decreases slightly with ionic strength in sodium chloride solutions. This might reflect systematic pH errors, or indicate that additional ion interaction parameters are required. To determine if such parameters are needed, a rigorous solution of the mean activity coefficient for $Cu(OH)_2$ was performed. Examination of this equation in Appendix A shows that only β_{CuOH} and ψ_{CuOHCl} would be affected by an increase in ionic strength. Their values reflect the linear dependence of the mean activity coefficient on the molal product of copper and chloride.

If β_{CuOH} and ψ_{CuOHCl} are necessary parameters a graph of the difference between the theoretical ln $\gamma^{\pm}$ $[Cu(OH)_2]$ required to obtain a constant ion activity product and the calculated ln $\gamma^{*\pm}[Cu(OH)_2]$ as a function of the molal product of copper and chloride in solution should be linear with an intercept at zero. To obtain the true activity coefficient, several calculations were required. The first step was to choose a predicted solubility product. Based on the intercept of the best fit line in Figure 3, $10^{-21.5}$ was chosen. Using this value, the calculated activity of

water, and the molalities of cupric and hydroxide ion, the theoretical $\gamma^{\pm}$ value could be calculated with the equation:

$$3\ln K + 3\ln(H_2O) - 3\ln(m_{Cu})(m^2OH) = \ln\gamma^{\pm}[Cu(OH)_2]$$

The difference between $\ln\gamma^{\pm}$ and $\ln\gamma^{*\pm}$ is given in Table 7. Figure 4 shows the relationship between the difference of mean activity coefficients and the molal product. No linear relationship was found, indicating there is no basis for fitting additional parameters for this system. Reexamination of the equations indicate that there must be concentration differences of either copper or hydroxide of several orders of magnitude before additional parameters such as β_{CuOH} or γ_{CuOHCl} are required.

The slight deviation from a horizontal line must therefore result from scatter in the data at high ionic strengths. This undoubtedly reflects pH measurement errors and not inadequacy of the ion interaction theory. If the error in the accuracy of the pH measurement were to vary linearly, an error of 0.05 units at 1m ionic strength and 0.15 units at 4m would be required to obtain a constant log ion activity product of -21.5 at 30°C. Our current inadequate understanding of pH measurement in brines does not justify such an interpretation of the data.

It is also possible that the tenorite and solution has equilibrated with atacamite ($Cu_4(OH)_6Cl_2$) in NaCl solutions.

Table 7. Difference in the theoretical $\ln^{*}\gamma\pm[Cu(OH)_2]$ needed to obtain a constant log Ksp = -21.5 at 30°C for the reaction; CuO (tenorite) + H_2O = Cu^{2+} + $2OH^-$ and the modeled $\ln\gamma\pm[Cu(OH)_2]$ as a function of the molal product of Cu^{2+} and Cl^- as discussed in the text. L and H are equivalent to the run numbers shown in Tables 5a and 5b while $\overline{X}$ is the average of those values.

Run#	L	H	$\overline{X}$	$(mCu^{2+})(mCl^-)$
1	-0.1551	-1.1752	-0.6652	5.60×10^{-8}
2	-3.3356	-3.3878	-3.3617	3.08×10^{-7}
3	-3.5663	-4.6659	-4.1161	5.63×10^{-7}
4	-6.1507	-6.1539	-6.1523	1.92×10^{-6}
5	-6.2168	-6.9839	-6.6004	3.15×10^{-6}
6	-9.2363	-7.9738	-8.6051	4.94×10^{-6}
7	-8.0571	-7.5543	-7.8057	10.08×10^{-6}
8	-8.5932	-8.2023	-8.3978	12.42×10^{-6}
9	-9.9398	-11.0419	-10.4909	15.50×10^{-6}
10	-6.2015	-6.3298	-6.2657	29.16×10^{-6}
11	-8.7346	-10.1034	-9.4190	54.22×10^{-6}

$\overline{X}$ is the average of L (low) and H (high) temperature experiments

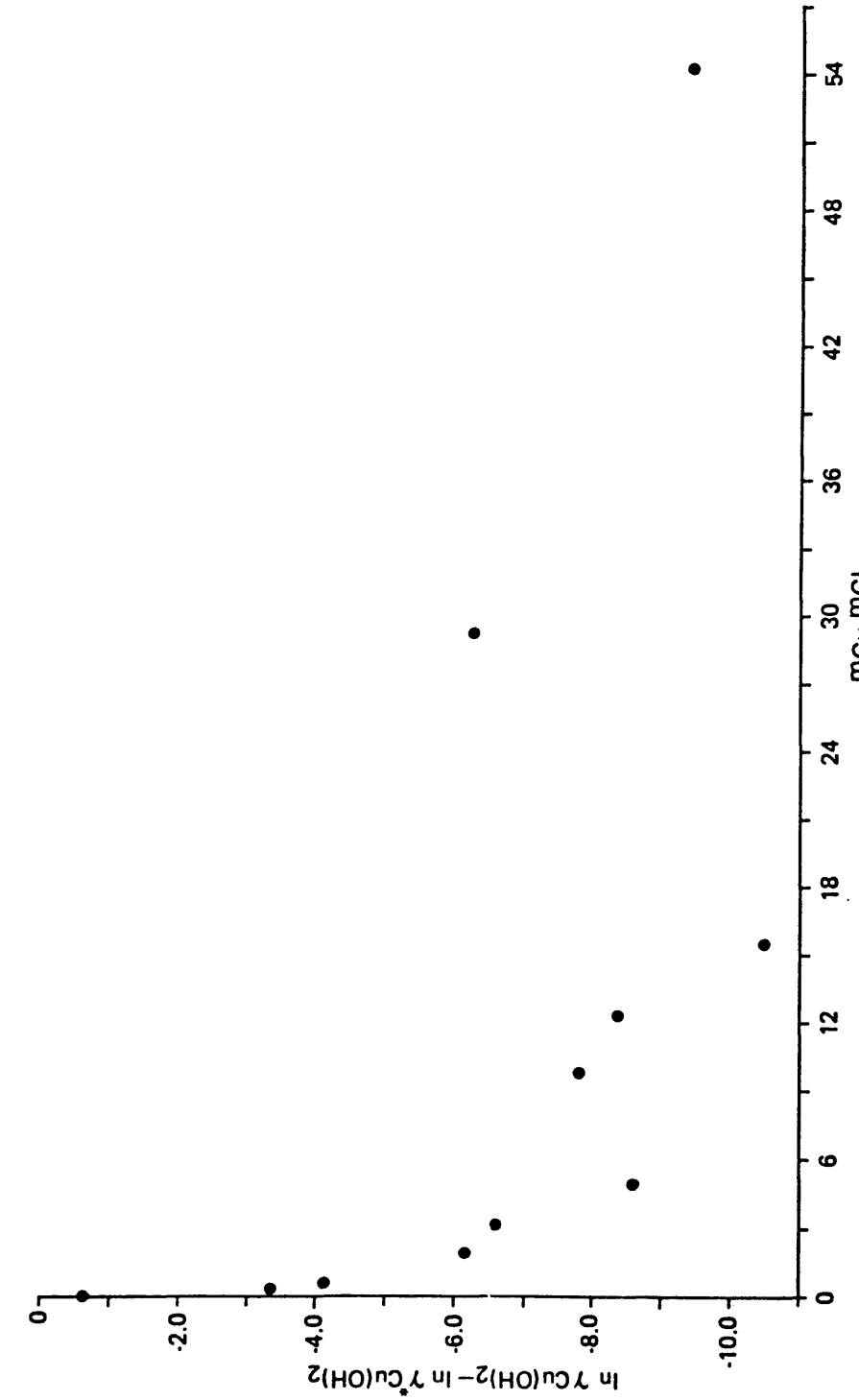

Figure 4. Theoretical mean activity coefficient of $Cu(OH)_2$ needed to obtain a constant log Ksp = -21.5 minus the calculated mean activity coefficient, plotted versus the molal product of Cu^{2+} and Cl^- ions for the NaCl experiments at 30° C. Data points are averages of the undersaturated and supersaturated runs.

Using the thermodynamic properties listed in Table 3 for the reaction:

$$4CuO + 2Cl^- + 4H_2O = Cu_4(OH)_6Cl_2 + 2OH^-$$

it can be shown that:

$$\log K = -6.7 \pm 0.8 = (OH^-)/(Cl^-)(H_2O)^2$$

Table 5 lists the calculated ion activity products for this reaction for each experiment. Figure 5 shows the calculated ion activity product as a function of sodium chloride molality. The plot shows the data crosses the calculated equilibrium constant. This indicates that the reaction can occur at low chloride concentrations, but suggests that the $(OH^-)/(Cl^-)$ activity ratio may decrease too quickly for atacamite to precipitate.

Based on a log K(tenorite) = -21.5, at 30°C, using a van't Hoff calculation to determine the change in log K at the two temperatures with an enthalpy of reaction of 14.0 kcal/mol yields log K = -21.7. This can be compared to the log solubility product of -21.9 for the Na_2SO_4 experiments. The average based on both sets of experiments is -21.8. This compares to log K(tenorite) = -19.7 and -20.6 based on Barton and Bethke (1960) and the data of Robie and others (1978) given in Table 3.

A comparison of the calculated ion activity quotients in Table 5 computed with and without the $CuCl_2$ virial

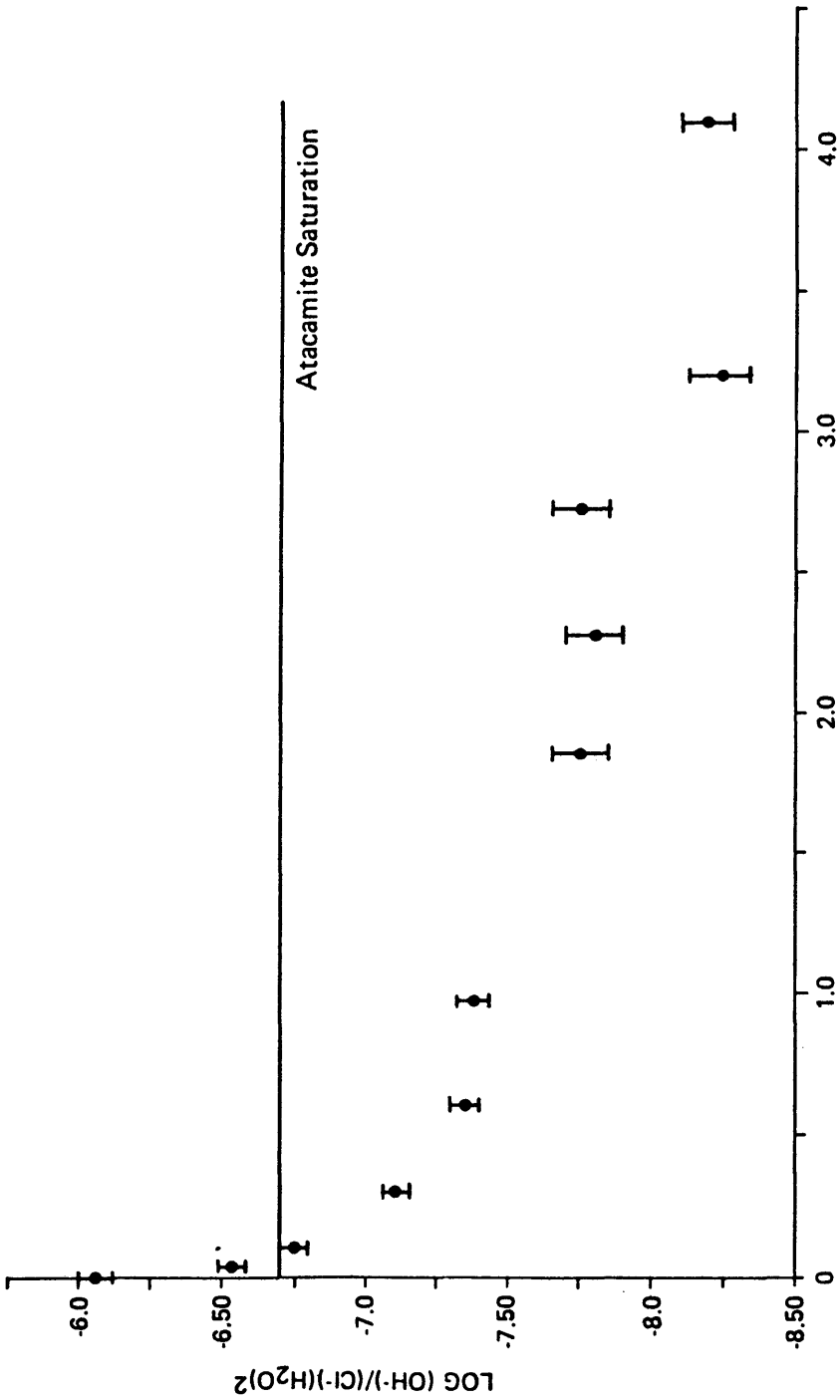

Figure 5. Calculated log ionic activity quotient for $4CuO + 4H_2O + 2Cl^- = Cu_4Cl_2(OH)_6 + 2OH^-$ versus I (NaCl) at 30° C. Data points are averages of undersaturated and supersaturated runs. Error bars are discussed in the text.

coefficients and mixing parameters reveals that they become increasingly significant above 0.05m. In other words, the calculated copper activity coefficient decreases more rapidly than it should with increasing ionic strength yielding an error in the log ion activity product of -1.5 at 4m NaCl. Thus the cupric chloride parameters are necessary to model cupric chemistry in chloride solutions above roughly 0.5 molal.

THE THERMODYNAMIC PROPERTIES OF BROCHANTITE

As was discussed earlier, the Na_2SO_4 experiments may have equilibrated with both brochantite and tenorite. The ΔG_f^o CuO at 25°C determined from these experiments is -32.6 ± 0.3 kcal/mol. From the experiments, for the reaction:

$$4CuO + SO_4^{2-} + 4H_2O = Cu_4SO_4(OH)_6 + 2OH^-$$

$$\log K > -14.0 \pm 0.1$$

Using the free energies listed in Table 3 for OH^-, SO_4^{2-}, and H_2O, the calculated free energy for brochantite is greater than or equal to -441.0 ± 0.4 kcal/mol versus -434.3 ± 0.6 given by Barton and Bethke (1960) for their finely crystalline solid. Based on an estimated entropy of 87.9 cal/K mol (Langmuir, 1983) and a Gibbs free energy of -441.0, the enthalpy of formation for brochantite would be greater than or equal to -527.4 kcal/mol.

MIXED ELECTROLYTE SYSTEMS

The solubility of tenorite in mixed electrolyte systems is of special relevance to the application of the ion interaction theory to natural systems. Accordingly, synthetic brines were prepared to model tenorite solubility in mixed electrolytes.

Four experiments were performed using the techniques discussed earlier, with the exception that the runs were held at 30°C for five weeks. Final run molalities, measured pH's, and thermodynamic pH's are recorded in Table 8.

Calculated ion activity products for tenorite are also given in Table 8 based on ion interaction modeling of the data. These products are well within the uncertainties discussed earlier for equilibration of tenorite. The ratio of $(OH^-)^2/(SO_4^{2-})$ is too high for tenorite to equilibrate with brochantite.

CONCLUSIONS

The importance of modeling the activity of trace metals in water has intensified recently in the light of interest in hazardous waste mobilities. Ion association models are inaccurate at ionic strengths much above 0.01-0.1m. The ion interaction model is currently under scrutiny to determine its usefulness in the modeling of

Table 8. Experimental and calculated activities of species present in four mixed electrolyte systems saturated with respect to tenorite at 30°C.

Table 8a. Molal concentrations of aqueous species present in each run and the measured (column a) and thermodynamic (column b) pH's.

Run	Na^+	K^+	Ca^{2+}	Mg^{2+}	$(Cu^{2+}) \times 10^6$	Cl^-	SO_4^{2-}	(a)	(b)
1	0.7900	0.0423	-	-	0.103	0.7693	0.0315	5.89	5.88
2	1.4228	-	-	0.0788	4.50	1.4228	0.0798	6.30	6.27
3	2.5354	0.0778	-	-	6.64	2.6132	-	6.16	6.11
4	2.5039	-	0.0380	-	8.37	2.5039	0.0380	6.31	6.26

Table 8b. Calculated ion and water activities for the mixed electrolyte systems, and log ionic activity quotients (column a) for dissolution of tenorite $CuO + H_2O = Cu^{2+} + 2OH^-$; and (column b) for the formation of brochantite $4CuO + SO_4^{2-} + H_2O = Cu_4SO_4(OH)_6 + 2OH^-$. The error in the log of the quotients is ± 0.1 for run 1 and ± 0.2 for the remaining runs.

Run	Na^+	K^+	Ca^{2+}	Mg^{2+}	(Cu^{2+}) x10^6	Cl^-	SO_4^{2-} (x10^3)	H_2O	(a)	(b)
1	0.496	0.0242	-	-	1.74	0.478	2.51	0.974	-21.7	-13.3
2	0.835	-	-	0.0177	0.692	0.903	3.60	0.951	-21.3	-12.7
3	1.61	0.0375	-	-	1.44	1.66	-	0.911	-21.3	-
4	1.56	-	0.0103	-	1.70	1.61	1.03	0.914	-20.9	-12.1

saline aqueous systems. Several studies have shown that such models can accurately determine the activities of major electrolytes and water up to six molal and above. Whether the same equations used for major electrolyte systems could accurately model trace metal chemistry had never before been addressed.

Until this study, no one had examined the solubility of a sparingly soluble, pH dependent mineral to assess the applicability of the ion interaction model. Tenorite solubility experiments were performed from pH range 5.8 to 6.5 in sodium chloride (0.009 to 4.1m), sodium sulfate (0.015 to 0.9m) and mixed electrolyte systems (0.8 to 2.6m). Where the values in parenthesis are stoichiometric ionic strengths. The results have been modeled with and without the published copper chloride and sulfate parameters. The calculated activity products showed the need for those parameters at ionic strengths above 0.05m in NaCl solutions.

Tenorite solubility runs in sodium sulfate solutions indicated that the solutions may have equilibrated with both tenorite and brochantite. The solubility in sodium chloride solutions was modeled up to four molal. The results were dependent on the measurement of pH which decreased in accuracy in solutions greater than one molal. Nevertheless tenorite solubility may be modeled up to four

molal sodium chloride, and in mixed electrolyte systems up to three molal ionic strengths.

More importantly, this study has shown that ion interaction equations and parameters may be used to model free trace metal ion activities when the latter are controlled by the solubility of rather insoluble minerals. Using an approach similar to the one used here, there is no reason why the activities of trace Ni, Li, Co, and Zn for example could not be accurately modeled with currently available interaction parameters.

RECOMMENDATIONS FOR FUTURE WORK

Before any additional experimental work on copper activity in waters is undertaken, this author firmly recommends that subsequent researchers closely examine the ion interaction equations. In natural systems, copper concentrations rarely exceed part per million concentrations, whereas concentrations of major electrolytes are several order magnitudes greater. Based on this fact, the effects of ion interactions on the activity coefficients of copper can be predicted without one ever entering the laboratory. With the ion interaction approach the effects of carbonate on cupric activity can probably be modeled using single ion activities, and assuming that the effects of mixing and

complexing are neglibible in the majority of natural systems.

The ion interaction approach to modeling the aqueous chemistry of natural waters is still in its infancy, but will probably become the standard approach, not only because of its accuracy, but because of its theoretical basis and mathematical simplicity. Future mineral solubility studies should be performed in different electrolytes as a function of ionic strength, and not simply at infinite dilution. The two approaches require the same level of effort yet the former provides us with a greater understanding of electrolyte behavior under a variety of conditions.

Another area of needed fundamental research is the measurement of pH in saline waters. Additional effort is required to understand the nature of processes that occur at the surface of glass electrodes in saline fluids.

PART II: THE THERMODYNAMICS AND GEOCHEMISTRY OF Ca, Sr, Ba, and Ra SULFATES IN SOME DEEP BRINES FROM THE PALO DURO BASIN, TEXAS

INTRODUCTION

Salt formations of the Palo Duro Basin of north Texas are being considered to host a repository for high-level radioactive waste. Candidate salt horizons are in the Lower San Andres Formation, which consists of five cycles of halite deposition. To establish the isolation of a repository site, the hydrogeology and geochemistry of the basin must be understood. The geochemistry of underlying deep basin aquifers is currently being investigated to assess the possible far-field impact of a repository breach. For this reason, the natural brines contained within the Wolfcamp Formation, underlying Pennsylvanian age carbonates and granite wash facies, are of interest.

Laul and other (1983) examined the activity ratios of dissolved natural uranium and thorium isotopes and their daughter products in Palo Duro brines. Bassett and Griffin (1981) found that two brine samples from the Wolfcamp Formation were at or near saturation with respect to gypsum and anhydrite using ion-interaction model calculations. However, no one to date has studied the solubility of Ca, along with Sr, Ba, and Ra sulfates, and the related

mobilities of Sr-90 and Ra-226, in these or other saline ground waters.

Previous studies of radionuclide ground water-mineral equilibria have employed an ion-association approach to calculate the activities of dissolved species (c.f. Garrels and Christ, 1965). The biggest limitation of the ion-association model at high ionic strengths is in the estimation of accurate ion activity coefficients. Computer program such as WATEQF (Plummer and others, 1976) and PHREEQE (Parkhurst and others, 1980) based on the ion-association approach obtain activity coefficients from the extended Debye-Hückel and Davies equations. These equations are inaccurate at ionic strengths much above 0.1 m, particularly for multivalent ions. Ionic strengths of brines in the Wolfcamp Formation and Granite Wash facies range from 2.89 to 4.76m. Thus, the ion-association approach is not applicable.

Pitzer (1973) developed the ion-interaction approach to determine the activity coefficients and osmotic pressures of electrolyte solutions. His equations are extensions of those proposed by Guggenheim (1935) and Pitzer and Brewer (1961) with modifications for higher ionic strengths developed by Scatchard (1939). Since 1973, Pitzer and his coworkers have extended the scope and

applications of the ion-interaction approach (Pitzer and others, 1974 a, b; and Pitzer 1975, 1979).

Harvie and Weare (1980) and Harvie and others (1982) employed ion-interaction equations to predict mineral equilibria in the $Na-K-Ca-Mg-SO_4-Cl-H_2O$ system at 25°C. They showed that the theoretical equations could accurately predict observed mineral solubilities at ionic strengths above 20 m. Gueddari and others (1983) used ion-interaction equations to examine the mineral/solution equilibria of the Chott El Jerid basin brines in southern Tunisia at ionic strengths up to 7.34m. They concluded that modeling results agreed with field observations. Millero (1983) estimated the ionization constants of weak acids in sea water using the ion-interaction approach. His study emphasized the interactions between Mg^{2+} and Ca^{2+} and weak acid anions.

Other than Bassett and Griffin (1981), no one has considered the geochemistry of deep brine aquifers or temperatures and pressures above 25°C and 1 bar using the ion-interaction approach. This study examines the geochemistry of Ca, Sr, Ba, and Ra sulfates in groundwaters in the Wolfcamp and Granite Wash aquifers in the Palo Duro Basin, Texas.

THE ION-INTERACTION APPROACH

Temperature and Pressure Corrections to the Ion-Interaction Model

A sample calculation was performed to establish the relative effect of temperature change on γ_{Ca}^{2+} caused by changes in the Debye-Hückel A_ϕ parameter, and in temperature derivatives of the ion interaction equations. For this purpose, a brine from the study area was modeled between 25 and 100°C. The equation of A_ϕ as a function of temperature (C) is: $A_\phi = 3.8 \times 10^{-6}t^2 + 4.724 \times 10^{-4}t + 0.3769$, for which the r^2 of fit is 0.99. Table 9 lists computed $\gamma_{Ca}2+$ values with temperature for the sample brine. The results indicate that the Debye-Hückel A_ϕ parameter correction is the most important one. The correction in $\gamma_{Ca}2+$ due to virial coefficient temperature derivatives never differs by more than 2% from that computed using A_ϕ alone. Thus, when the temperature derivatives for virial coefficients are unknown, they can generally be ignored up to 100°C.

To model deep brine aquifers, the effect of pressure must also be considered. Pitzer (1979) examined temperature and pressure effects on the virial coefficients and concluded that only the temperature contribution was signi-

ficant. Rogers (1981) has similarly shown that the A_ϕ parameter deviates a maximum of three percent over a pressure range of 1 to 600 bars. The greatest pressure measured in this study was 130 bars. Thus, the effect of pressure on ion activities can be ignored.

Alkaline Earth Sulfate Modeling

The thermodynamic relationships for $CaSO_4$, $SrSO_4$, and $BaSO_4$ in simple electrolyte solutions at 25°C were examined by Rogers (1981). Her study indicated that the virial coefficients and mixing parameters for $CaSO_4$ could accurately be extended to $SrSO_4$ and $BaSO_4$ in simple electrolyte systems. Using the same approach in this study, the virial coefficients and mixing parameters necessary to model $RaSO_4$ in electrolyte solutions were assumed equal to those for $CaSO_4$. Other Ra electrolyte parameters were taken equal to the corresponding Ca values.

THE THERMODYNAMIC DATA BASE

Solubility Products of Ca, Sr, Ba and Ra Sulfates

In order to establish the saturation state of the study area ground waters with respect to sulfate minerals it was necessary to define solubility products of the sulfates as a function of temperature and pressure. As

Table 9. Relative effects on $\gamma_{Ca^{2+}}$ for a typical brine, of the Debye-Hückel A_ϕ parameter and of the ion interaction (I-I) expressions as a function of temperature.

T(°C)	A_ϕ temp. effect $\gamma_{Ca^{2+}}$	A_ϕ temp. plus I-I effects $\gamma_{Ca^{2+}}$
25	.249	.247
30	.240	.241
40	.223	.224
50	.205	.207
60	.187	.189
70	.170	.172
80	.153	.155
90	.136	.139
100	.121	.123

shown in Table 10, ground water temperatures ranged from 32 to 41°C and pressures from 67 to 130 bars.

Blount (1977) measured the solubility of barite in aqueous solutions up to 4 molal NaCl, at temperatures from 22 to 280°C, and pressures from 1 bar to 1400 bars. His equation for the solubility product of barite as a function of temperature (K) and pressure (bars) is

$$\log K_{sp}(\text{barite}) = (1.49325\times10^{-2}P - 48.61)\log T + (2.35365P - 7682.76)T^{-1} - 4.398\times10^{-2}P + 136.079$$

At 1 bar pressure this reduces to

$$\log K_{sp}(\text{barite}) = 136.035 - 7680.41T^{-1} - 48.595\log T$$

This equation yields log Ksp (barite) = -9.97 at 25°C, in good agreement with our preferred value of -9.96 (Rogers, 1981). Blount's molal solubility results in water from 25 to 175°C at 1 bar below 100°C, and on the liquid-vapor curve above 100°C were modeled with the ion-interaction algorithm. Resultant log Ksp values were within ± 0.02 units of the values computed with the above equation between 25 and 175°C. The difference between log Ksp values computed with the two equations given above indicates that the effect of hydrostatic pressures in study area ground waters ranges from +0.06 to +0.10 units in log Ksp (barite), increasing with increasing pressure.

Table 10. Well water temperatures and pressures, and well completion information.

Well	Formation or Facies	Zone	Land surface elevation(m)	Depth of ground water sampling interval (m)	T(°C)	P(bars)
Sawyer 1	Wolfcamp	5	786	- 967 to - 972	32	67
Sawyer 1	granite wash	4	786	-1298 to -1323	38	93
Mansfield 1	Wolfcamp	1	1126	-1469 to -1491	40	101
Mansfield 1	Wolfcamp	2	1126	-1376 to -1414	39	79
Zeeck 1	Wolfcamp	3	1040	-1667 to -1692	38	130

The solubility of gypsum at 25° is 0.0154 ± 0.0002 mol/kg based on the average of 14 independent solubility measurements given by Seidell (1958). Ion pairing model calculations with an association constant log K of 2.31 for the $CaSO_4^o$ ion pair (Bell and George, 1953), Debye-Hückel ion activity coefficients for Ca^{2+} and SO_4^{2-}, and assuming log $CaSO_4^o$ = -0.45I (Reardon and Langmuir, 1974) leads to log Ksp(Gypsum) = -4.59. The same value was adopted by Rogers (1981). Blount and Dickson (1973) give an equation for the molal solubility of gypsum based on their own solubility measurements from about 40° to 83°C at pressures up to 1000 bars, and the work of others between 0 and 90°C in the same pressure range. At 25°C their equation yields a gypsum solubility of 0.0152 mol/kg. This corresponds to log Ksp (gypsum) = -4.58 based on ion-interaction calculations. Log Ksp(gypsum) values for 25 to 90°C at 1 bar computed from Blount and Dickson's solubility equation fit the expression:

$$\log Ksp(gypsum) = 68.2401 - 3221.51T^{-1} - 25.0627\log T$$

where T is in Kelvin. This equation reproduces ion-interaction modeled log Ksp values in this temperature range to within ± 0.005 units or better.

Considerable disagreement has existed over the temperature of gypsum-anhydrite equilibrium at 1 bar and unit

activity of water. Blount and Dickson (1973) summarize the literature on this subject, most of which supports a temperature of about 40-42°C. Their own work suggests an equilibrium temperature of 56 ± 3°C in good agreement with Hardie (1967) whose careful solubility measurements indicate a temperature of 58 ± 2°C. We will assume 56°C is the correct transition temperature in this study. It must be pointed out, however, that no one has successfully reversed solubility measurements on anhydrite below about 70°C (Blount and Dickson, 1973), the gypsum-anhydrite transition temperature, and anhydrite solubilities below 70°C have of necessity been obtained by extrapolation of higher temperature data.

Blount and Dickson's (1973) molal solubility measurements on anhydrite above 95°C which they combined with such measurements by other observers in a general equation, have been modeled with the ion interaction algorithm from 25 to 150°C. Values below 56°C were not considered in the fit because they are only estimates obtained by extrapolation from higher temperature via Blount and Dickson's equation. The results, which are given in column 2 of Table 11, have been fit with the equation:

$$\log K_{sp}\ (\text{anhydrite}) = 87.805 - 3210.8T^{-1} - 32.846\log T$$

Table 11. The solubility product (-logKsp) of anhydrite from 25 to 150°C at 1 bar: (1) computed from the molal solubility equation of Blount and Dickson (1973) using the ion-interaction (I-I) model; (2) computed from an equation fit to the I-I model derived values between 56 and 150°C; and (3) based on the barite-anhydrite exchange reaction at 56°C assuming ΔC_p constant (from Langmuir, 1984).

T(°C)	(1) I-I model	(2) Equation fit to I-I values	(3) Barite anhydrite reaction
25	4.19	4.24	4.26
30	4.26	4.30	4.31
40	4.41	4.42	4.43
50	4.55	4.56	4.56
56	4.64	4.64	4.64
60	4.69	4.69	4.70
75	4.91	4.90	4.93
100	5.28	5.28	5.34
125	5.65	5.66	5.79
150	6.05	6.05	6.26

where T is in Kelvin. Between 40 and 150°C values obtained with this equation lie within ± 0.01 log units of those computed by ion-interaction modeling (see Table 11). However, at lower temperatures they diverge, differing by 0.05 log units at 25°C.

At 56°C, log Ksp (gypsum) = log Ksp (anhydrite) = 4.64 based on ion interaction modeling of Blount and Dickson's solubility of 0.01505 mol/kg. With ΔH° = 1650 cal/mol and log K = -2.31 for dissociation of the $CaSO_4^\circ$ ion pair at 25°C (Bell and George, 1953), and the van't Hoff equation, we can predict log K = -2.42 for the ion pair at 56°C. Ion-pairing model computations carried out as described above for gypsum, lead to log Ksp (anhydrite) = -4.65_5 at 56°C, in good agreement with -4.64 obtained with the ion interaction model.

An independent approach was taken by Langmuir (1984) to obtain log Ksp (anhydrite) based on the fact that the heat capacity (ΔC_p°) of this reaction,

$$Ca^{2+} + BaSO_4(c) = Ba^{2+} + CaSO_4(c)$$

is constant, as a function of temperature, using the "Principle of Balance of Identical Like Charges" (c.f. Murray and Cobble, 1980). Heat capacities for the ions from Helgeson and others (1981), and for the solids from Parker and others (1971) lead to ΔC_p° = -5.1 cal/mol deg.

Entropies from Parker and others (1971) result in ΔS_r° = 8.9 cal/mol deg for the reaction at 25°C. ΔG_r° = -7.64 kcal/mol at 25°C based on the solubility products of barite and anhydrite. At 56°C, log Ksp (anhydrite) = -4.64 and ΔG_r° = 7518 cal/mol. Assuming ΔC_p° = -5.1 cal/mol deg, Langmuir then computed ΔS° = 8.78 cal/mol deg at 56°C, which led to the function,

$$\Delta G^\circ = 12086.6 - 43.442T + 11.743T\log T$$

for the barite-anhydrite reaction, where T is in Kelvin. We also know that

$$\Delta G^\circ = -RT\ln[Ksp(barite)/Ksp(anhydrite)]$$

Combining above equations and simplifying leads to

$$\log Ksp(anhydrite) = 126.722 - 5098.61T^{-1} - 46.029\log T$$

In Table 11, log Ksp values computed from this function are compared to values obtained by ion-interaction modeling, data and those obtained with the equation fit to the solubility data of Blount and Dickson (1973). The difference between values derived from the fitting equation and above equation from the barite-anhydrite reaction is ± 0.02 log units or less from 25 to 60°C, but increases at lower and higher temperatures. Based on these two largely independent approaches, it seems likely that at 25°C log Ksp(anhydrite) is closer to -4.25 than -4.19. If this is

correct, then for the dehydration reaction

$$CaSO_4 \cdot 2H_2O = CaSO_4 + 2H_2O$$

given log Ksp(gypsum) = -4.58 and log Ksp(anhydrite) = -4.25, we can show ΔG° = 450 cal/mol, and $[H_2O]$ = 0.68 at 25°C. This compares at the same temperature to ΔG° = 273 cal/mol computed from free energy data given by Robie and others (1978), and ΔG° = 294 cal/mol and $[H_2O]$ = 0.78 at equilibrium (see Berner, 1971). The last two free energy values are apparently based on Hardie's (1967) results.

The equations given by Blount and Dickson (1973) for the molal solubilities of gypsum and anhydrite were used to calculate the combined effects of temperature and pressure on log Ksp values for both minerals in the ground water as follows. Molal solubilities for T and P conditions given in Table 10 were computed with Blount and Dickson's (1973) equations. The results were input into the ion-interaction algorithm to derive the necessary log Ksp values. Results showed that the pressure effect on log Ksp (gypsum) ranged from + 0.030 to + 0.056, and the effect on the log Ksp (anhydrite) from + 0.039 to + 0.075, with values increasing with pressure in both cases.

Strübel (1966) measured the solubility of celestite between 20 and 600°C, at ionic strengths up to 2m NaCl, and pressures up to 2000 bars. His data below 100°C for 1 bar

were modeled with the ion-interaction algorithm. Resultant log Ksp values were fit with the equation

$$\log Ksp(celestite) = 137.555 - 6530.75T^{-1} - 49.4198\log T$$

where T is in Kelvin. The average deviation of this equation from the log Ksp values is ± 0.01 units, and the maximum deviation ± 0.02 units. At 25°C log Ksp computed from the above equation is -6.63_5, close to -6.60, the value proposed by Rogers (1981).

Reardon (1983) obtained an average solubility of 6.60 ± (0.05×10^{-4}) molal for celestite in water at 25°C based on four reversed runs. This value was input into the ion-association model and also into an ion-pairing model calculation. Log Ksp values so obtained were -6.60 and -6.62, respectively.

MacDonald and North (1974) examined the effect of pressures up to 1000 bars on celestite solubility at 0, 22 and 35°C. Their measurements show that the pressure effect on log Ksp(celestite) is nearly independent of temperature between 2 and 35°C. At 35°C, in the temperature range of study area ground waters, Langmuir (1984) found their data for 50 to 1000 bars fit the relation $d\log Ksp/dT = 8.576 \times 10^{-4}P$, with $r^2 = 1.00$ for the fit. This function indicates that log Ksp(celestite) increases with pressure,

and that the pressure effect on log Ksp ranges from +0.06 to +0.11 for study area ground waters.

A constant heat capacity of reaction approach similar to that used to calculate log Ksp (anhydrite) was taken by Langmuir (1984) to determine the effect of temperature on Ksp($RaSO_4$). For the reaction

$$BaSO_4(c) + Ra^{2+} = RaSO_4(c) + Ba^{2+}$$

with enthalpy and free energy data from Langmuir and Riese (1984), ΔG_r° = - 396 cal/mol, ΔH_r° = 3050 cal/mol, and thus ΔS_r° = 8.9 cal/mol deg. Assuming ΔC_p° = 0, independent of temperature, leads eventually to

$$\Delta G_r^\circ = - 3049.5 + 8.9T$$

for the above reaction. Substituting for log Ksp(barite) as before, Langmuir (1984)

$$\log Ksp(RaSO_4) = 137.98 - 8346.87T^{-1} - 48.595\log T$$

The effect of pressure on log Ksp($RaSO_4$) was assumed equal to that effect for barite.

To interpret the solubility modeling results, the ion-activity product (IAP) of each mineral is compared to its solubility product for ground water conditions. The logarithm of their ratio is called the saturation index (SI). Thus SI = log (IAP/Ksp). There is no precedence for

defining a range of SI values around saturation (SI = 0) within which range we can assume all values are at saturation. The fact that computed SI values for such minerals as anhydrite are often within a few hundredths of a log unit of zero indicates that cumulative uncertainties in the ion-interaction calculations are either compensating, or small. Jenne and others (1980) somewhat arbitrarily chose an error band of ± 1/20th of log Ksp to indicate a water's saturation with respect to a mineral. We have adopted their convention for this study for lack of a more rigorously defensible approach.

Radium Solid Solutions

Langmuir and Riese (1984) note that Ra concentrations in ground water are always too low to reach saturation with respect to a pure Ra phase of which $RaSO_4(c)$ is the least soluble. Radium concentrations instead are limited either by adsorption or by solid solution formation or both. Radium adsorption is inhibited by low pH's and by high concentrations of other dissolved cations, especially Ca, because of competition with Ra for adsorption sites (Riese, 1982). The Wolfcamp and granite wash brines have low pHs (4.4 to 6.3) and are high in Ca (0.188 to 0.481m). The Wolfcamp and granite wash are low in clays and other minerals such as the Fe and Mn oxyhydroxides which have

high adsorption capacities. Thus, we can expect adsorption is not a major control on Ra concentrations.

As is discussed in more detail later, maximum concentrations of Ca, Sr, and Ba in the ground water are limited by the solubilities of anhydrite or gypsum, celestite and barite. However, Ra concentrations are always considerably lower than saturation with respect to pure $RaSO_4$. Instead, maximum Ra concentrations are apparently limited by the solubility of trace Ra solid solutions in celestite and barite, and to a minor extent in anhydrite or gypsum, calcite, and dolomite.

Langmuir and Riese (1984) concluded that the solubility of radium in sulfate and carbonate minerals decreases with increasing temperature. For example, a temperature increase from 25 to 100°C reduces the solubility of radium in anhydrite, aragonite, barite and celestite, by 18, 3.4, 2, and 9.3 times, respectively.

It must be emphasized that these calculations are for a compositionally homogeneous solid solution; one formed instantaneously from a water of constant composition, without significant decay of Ra-226 in the solid solution to its daughter products (Ra-226 half-life 1622 y). Such conditions may be approached in the vicinity of a breached high level nuclear waste repository, when sulfates or car-

bonates are precipitated, but are not applicable to the Ra geochemistry of most natural water-rock systems where Ra-226 is chiefly derived from the radioactive decay of U-238.

WATER SAMPLING AND CHEMICAL AND ISOTOPIC ANALYSTS

Sample Collection and Preservation

During the drilling of wells sampled in this study, a thiocyanate tracer was added to the drilling fluid. Prior to sample collection, all wells were pumped continuously until the quantity of thiocyanate tracer in the ground water decreased to 0.5% or less of its original concentration (Hubbard, 1984). Water samples were collected at the surface discharge point. All samples collected for radionuclide analysis were passed through multiple 0.3 micron filters and acidified with reagent grade nitric acid. Samples collected for Ra analyses were collected by passing spiked Ba-133 water through multiple filters (0.3 micron) and beds of Al_2O_3 impregnated with $BaSO_4$. All samples collected for the chemical analysis of major and minor dissolved species were field filtered through 0.45 micron filters and acidified with nitric acid.

Physical, Chemical and Isotopic Measurements

All physical and chemical measurements were made by Bendix Field Engineering Corporation, Grand Junction, CO. Ra-226 measurements were done by Laul and others (1983).

Formation temperatures were measured with a downhole thermistor. Unfortunately no measure of accuracy was made yet the values reported are probably accurate to ± 1°C. The downhole hydrostatic pressure was determined using a piezometer and, again, no measure of accuracy was made, yet the values reported are probably accurate to within ± 2%. Formation pressures and temperatures are listed in Table 10. Hydrostatic pressures are lower than expected for wells at such depths because the ground water table is about three hundred meters below the land surface.

Table 12 lists the chemical analytical methods used to determine the concentrations of dissolved species. Major species concentrations are considered accurate to within ± 10% or better (Chessmore, 1983). Table 13 gives the molalities, and modeled activity coefficients and activities of the major and minor species including Ra-226 in each brine.

Table 12. Summary of methods of chemical and isotopic analysis and their detection limits.

Species	Analytical Methods	Detection limits in ppm unless otherwise indicated[a]
Na	Atomic absorption	0.05
K	Atomic absorption	0.05
Ca	Atomic absorption	0.1
Mg	Atomic absorption	0.01
Sr	Inductively coupled plasma	0.05
Ba	Inductively coupled plasma	0.1
Ra-226	γ-counting using a low energy photon detector	0.1 pCi/l
Cl	Specific ion electrode	2.0
SO_4	Ion chromatography	5.0
Br	Energy dispersive x-ray	0.6

[a] Based on discussions with R. Chessmore and for Br the work of Kubo and others (1978).

Table 13. Molal concentrations (m), activity coefficients (γ), activities (a), and other chemical properties of the well waters, including field pH, stoichiometric ionic strengths (I) and osmotic coefficients (ϕ). All major element analyses are from Bendix Field Engineering Corporation, Grand Junction, CO; Ra analyses from Hubbard (1984).

	Sawyer Well 1* Wolfcamp Aquifer			Sawyer Well 1* Granite Wash Aquifer		
Species	m	γ	a	m	γ	a
Na	1.88	0.646	1.21	2.68	0.753	2.02
K	3.62×10^{-3}	0.480	1.74×10^{-3}	9.91×10^{-3}	0.454	4.50×10^{-3}
Ca	0.188	0.237	4.45×10^{-3}	0.516	0.402	2.08×10^{-1}
Mg	0.123	0.303	3.73×10^{-2}	0.113	0.587	6.63×10^{-3}
Sr	1.68×10^{-3}	0.204	3.42×10^{-4}	7.37×10^{-3}	0.329	2.42×10^{-3}
Ba	7.64×10^{-7}	0.156	1.19×10^{-7}	1.10×10^{-5}	0.198	2.18×10^{-6}
Ra	4.6×10^{-12}	0.156	7.2×10^{-13}	1.5×10^{-12}	0.198	3.0×10^{-13}
Cl	2.53	0.790	2.00	4.25	0.982	4.17
SO_4	2.35×10^{-2}	0.037	8.71×10^{-4}	7.85×10^{-3}	0.024	1.88×10^{-4}
Br	5.16×10^{-3}	0.908	4.69×10^{-3}	7.64×10^{-3}	1.226	9.36×10^{-3}
H_2O			0.914			0.847
	pH = 6.1 I = 2.89 ϕ = 1.049			pH = 4.4 I = 4.76 ϕ = 1.211		

* Sr and Ba analyses from an independent laboratory.
** Ba analysis from an independent laboratory.

Table 13. (continued).

Species	Mansfield Well Zone 1** Wolfcamp Aquifer m	γ	a	Mansfield Well Zone 2 Wolfcamp Aquifer m	γ	a
Na	3.70	0.739	2.74	3.74	0.741	2.77
K	1.45×10^{-2}	0.463	6.77×10^{-3}	1.56×10^{-2}	0.462	7.21×10^{-3}
Ca	0.242	0.339	8.20×10^{-2}	0.242	0.347	8.40×10^{-2}
Mg	8.20×10^{-2}	0.477	3.91×10^{-2}	8.50×10^{-2}	0.491	4.18×10^{-2}
Sr	1.60×10^{-3}	0.281	4.50×10^{-4}	1.49×10^{-3}	0.286	4.26×10^{-4}
Ba	6.59×10^{-7}	0.171	1.13×10^{-7}	1.59×10^{-6}	0.173	2.76×10^{-7}
Ra	1.5×10^{-12}	0.171	2.5×10^{-13}	1.2×10^{-12}	0.173	2.0×10^{-13}
Cl	3.95	0.961	3.80	3.99	0.966	3.85
SO_4	1.39×10^{-2}	0.029	3.99×10^{-4}	1.54×10^{-2}	0.028	4.37×10^{-4}
Br	1.47×10^{-3}	1.209	1.78×10^{-3}	1.64×10^{-3}	1.216	1.99×10^{-3}
H_2O			0.845			0.843
	pH = 5.6 I = 4.51 ϕ = 1.172			pH = 4.8 I = 4.56 ϕ = 1.175		

Table 13. (continued).

Species	Zeeck Well Zone 3 Wolfcamp Aquifer m	γ	a
Na	3.29	0.718	2.36
K	1.10×10^{-2}	0.475	5.22×10^{-3}
Ca	0.175	0.314	5.49×10^{-2}
Mg	8.60×10^{-2}	0.430	3.70×10^{-2}
Sr	1.68×10^{-3}	0.262	4.40×10^{-4}
Ba	7.81×10^{-8}	0.172	1.34×10^{-8}
Ra	2.3×10^{-12}	0.172	4.0×10^{-13}
Cl	3.55	0.882	3.13
SO_4	1.79×10^{-2}	0.031	5.46×10^{-4}
Br	6.05×10^{-3}	1.078	6.52×10^{-3}
H_2O			0.865

pH = 6.3
I = 3.99
ϕ = 1.130

GEOLOGY AND HYDROLOGY OF THE WOLFCAMP FORMATION AND GRANITE WASH FACIES

The Wolfcamp Formation and granite wash facies are located in the Palo Duro Basin in the Texas Panhandle and in early Permian eastern New Mexico (Figure 6). The granite wash, of Pennsylvanian age, is composed of coarse arkosic sands and gravels deposited in deltaic fans adjacent to uplifted areas. The sediments are interbedded with marine carbonates and terrigenous muds. The Wolfcamp Formation of early Permian age, formed during a period of regional uplift. Subsequent subsidence yielded conditions favorable for the growth of reef-forming and shelf carbonates. Arid climate allowed continual evaporation with the deposition of large amounts of evaporite minerals (Gustavson and others, 1979). The Wolfcamp Formation is predominantly limestone and dolomite along the basin margins, grading in the central part of the basin into thick units of limestone and dolomite interbedded with black shales. A detailed petrographic and mineralogical analysis of core material from the Wolfcamp was performed by Fukui (1983). He did not find celestite, barite, or a discrete radium mineral in any of the cores. This is not surprising in that celestite and barite would likely occur as less than 1% of the sample, and no radium minerals exist. Anhydrite

was visible only in vugs from a core from the Mansfield well and did not exhibit any dissolution features.

The Wolfcamp Formation is overlain by the Leonard, Guadalupe, and Ochoa units, which contain thick anhydrite beds along with dolomite and halite (Bentley, 1981). Kushnir (1980) points out that the alteration of gypsum to anhydrite as has occurred in this overlying sequence, leads to the precipitation of celestite unless the water of hydration of the gypsum is diluted.

Large pockets of highly saline water are present in the Wolfcamp and granite wash. Bentley (1981) showed that ground water flow in both formations is to the east and northeast. He also suggested that the evaporite sequences associated with the Wolfcamp and granite wash act as aquicludes, limiting the vertical flow of formation waters. Located in Figure 6 are wells from which brine samples were obtained for this study.

GEOCHEMISTRY OF THE BRINES

General Ground Water Chemistry

This section discusses the ground water chemical characteristics of water from the Wolfcamp and granite wash. Sawyer Well water was collected from both the Wolfcamp and granite wash. Table 10 provides information on the depth intervals sampled. Waters from both zones are Na-Cl brines

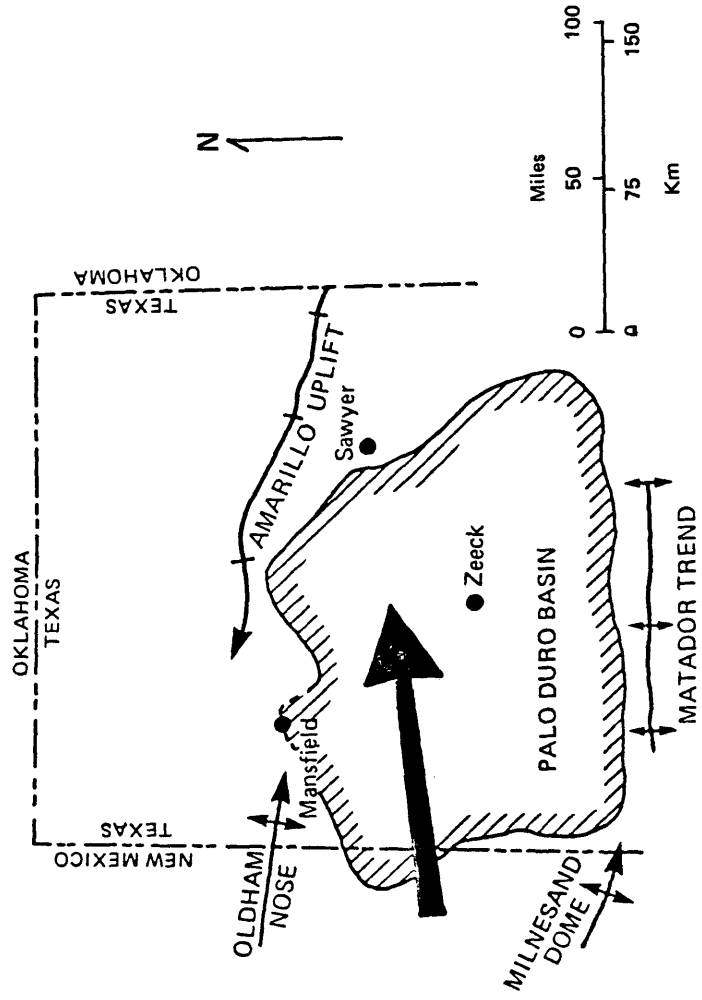

Figure 6. Well locations in the Palo Duro Basin. Arrow indicates general ground-water flow direction within the Wolfcamp Formation.

that contain relatively high concentrations of Ca, Mg, Sr, Br and SO_4 with water from the granite wash having higher levels of most of these species. The pH's differ by 1.7 units between the aquifers, for unknown reasons. The pH throughout the Wolfcamp is undoubtedly buffered by the carbonates present.

Water was collected from two zones from the Mansfield Well. The waters from these zones are Na-Cl brines with high Ca and SO_4 concentrations. Even though there is 50m separating the deepest extent of zone 1 from the top of zone 2 the water chemistries are remarkably similar with the exception of the measured pH.

The Zeeck Well is located in the central part of the basin where the Wolfcamp contains carbonates interbedded with black shales. Slightly elevated organic carbon contents in the central part of the basin relative to the basin margins may have led to aqueous sulfate reduction, but has not otherwise changed the chemical characteristics of the water, which is a Na-Cl brine containing high concentrations of Ca and Br.

DISCUSSION OF MINERAL SATURATION INDICES

Mineral saturation indices (SI's) are representative of the mineralogic control of water chemistry. Since mineral solution equilibria may control the ionic com-

position of water, a detailed model is warranted. In this study, waters from the Wolfcamp carbonates and arkosic granite wash were examined to understand their sulfate equilibria. Unfortunately, only five waters were available; yet they should provide a sufficient field test for the ion-interaction model.

The SI's presented in Table 14 for all the five waters indicate saturation of the five with gypsum, anhydrite, and celestite and three of the five with barite. $RaSO_4$ is undersaturated in all the waters.

The saturation results for $RaSO_4$ are consistent with the findings of Langmuir and Riese (1984) who argue that no natural water is saturated with $RaSO_4$. Instead it is likely that the aqueous Ra has equilibrated as a trace solid-solution with a major sulfate mineral.

Except for the presence of trace amounts of anhydrite in vugs in the Mansfield, none of the minerals found saturated in the water were found in the cores. In addition, the anhydrite showed no evidence of dissolution features (Fukui, 1984), indicating it was formed well after deposition of the Wolfcamp and is the stable $CaSO_4$ mineral phase, not gypsum. Gypsum was probably the stable phase under depositional conditions, but became unstable later as

Table 14. Mineral saturation indices for the five ground waters. The ± values shown in parentheses below the mineral names are the permissible range of SI values within which a water is considered saturated with respect to that mineral. See text.

Mineral	Sawyer Well Wolfcamp	Sawyer Well Granite Wash	Mansfield Well Zone 1 Wolfcamp	Mansfield Well Zone 2 Wolfcamp	Zeeck Well Zone 3 Wolfcamp
Anhydrite (± 0.2)	-0.12	-0.06	-0.12	-0.07	-0.20
Gypsum (± 0.2)	+0.07	0.00	-0.08	-0.02	-0.11
Celestite (± 0.3)	+0.05	+0.22	-0.19	-0.16	-0.09
Barite (± 0.5)	-0.17	+0.34	-0.65	-0.20	-1.44
$RaSO_4$ (± 0.5)	-5.1	-6.3	-6.1	-6.1	-5.8

indicated by the mineralogy of the overlying units. The present water chemistry is probably influenced by the mineralogy of the overlying Leonard and Ochoa units which contain thick beds of halite and anhydrite, and/or by dissolution of evaporite units near the recharge zone where they probably also contain celestite and barite. Further support for this hypothesis might be provided by comparisons of aqueous Br and I in the Wolfcamp brines with their concentrations in the Leonard and Ochoa evaporites (c.f. Kreitler and others, 1983).

CONCLUSIONS

Ion-interaction theory has been used to predict mineral/solution equilibria for Ca, Sr, Ba, and Ra-SO_4 minerals in the Wolfcamp Formation and granite wash facies, Palo Duro Basin, Texas. The equations have accurately modeled waters with ionic strengths ranging from 2.9 to 4.6 molal and temperatures up to 41°C.

In conclusion:

(1) The A_ϕ parameter is the most important correction needed for modeling the effect of temperature on ion activity quotients up to 100°C.

(2) Several waters from all of the basin are saturated with respect to gypsum, anhydrite, celestite, and usually barite.

(3) None of the waters are saturated with $RaSO_4$.

(4) Aqueous chemistry of the Wolfcamp and granite wash have resulted from the interaction with the overlying Leonard and Ochoa units.

(5) Ion-interaction equations and parameters may be used to accurately model the activities of major ion electrolytes in deep brine systems at elevated temperatures.

REFERENCES CITED

Barton P. B. and Bethke P. M. (1960) Thermodynamic properties of some synthetic zinc and copper minerals. Am. J. Sci. 258-A, 21-34.

Bassett R. L. and Griffin J. A. (1981) AQ/SALT: Calibration of a brine model in Geology and Geohydrology of the Palo Duro Basin, Texas Panhandle. Geol. Circ. 81-3, 146-152.

Bates R. (1964) Determination of pH, theory and practice. Wiley.

Bell R. P. and George J. H. B. (1953) Dissociation of phallous and Ca sulfate salts at different temperatures. Trans. Farad. Soc., 49, 619-627.

Bentley M. E. (1981) Regional hydaulics of brine aquifers, Palo Duro and Dalhart basins, Texas. In, Geology and geohydrology of the Palo Duro Basin, Texas Panhandle - a report on the progress of nuclear waste isolation feasibility studies (1980). The Univ. Texas at Austin, Bur. Econ. Geology Geological Circ. 81.

Berner R. A. (1971) Principles of Chemical Sedimentology. McGraw-Hill.

Blount C. W. (1977) Barite solubilities and thermodynamic quantitites up to 300°C and 1400 bars. Am. Min. 62, 942-957.

Blount C. W. and Dickson F. W. (1973) Gypsum-Anhydrite equlibria in systems $CaSO_4$-H_2O and $CaSO_4$-NaCl-H_2O. Am. Min. 58, 323-331.

Bockris J. O'M. and Reddy A. K. (1977) Modern Electrochemistry. Plenum/Rosetta.

Butler G. P. (1973) Strontium geochemistry of modern and ancient calcium sulphate minerals. In: The Persian Gulf (B. H. Purser editor) Springer, 423-452.

Chessmore R. (1984) Personal communications, Bendix Field Engineering Corporation, Grand Junction, CO.

CODATA Task Group on Key Values for Thermodynamics (1976) Recommended Key Values for Thermodynamics. 1975. J. Chem. Thermodyn. 8, 603-605.

CODATA Task Group on Key Values for Thermodynamics (1977) Recommended Key Values for Thermodynamics, 1976. J. Chem. Thermodyn. 9, 705-706.

Downes C. J. and Pitzer K. S. (1976) Thermodynamics of electrolytes. Binary mixtures formed from aqueous NaCl Na_2SO_4, $CuCl_2$, and $CuSO_4$ at 25°C. J. Sol. Chem. 5(6), 389-398.

Duby P. (1977) The thermodynamic properties of aqueous inorganic copper systems, INCRA Monograph IV The metallurgy of copper.

Feitknecht W. and Schindler P. (1963) Principles of the determination of solubility constants of hydroxide precipitates. Pure Appl. Chem. 6, 130-199.

Fukui L. (1983) Written Communication, Bendix Field Engineering Corporation, Grand Junction, CO.

Garrels R. M. and Thompson M. E. (1962) A chemical model for sea water at 25°C and one atmosphere total pressure. Am. J. Sci. 260, 57-66.

Gueddari M., Monnin C., Perret D., Fritz B., and Tardy Y. (1983) Geochemistry of brines of the Chott El Jerid in southern Tunisia - Application of Pitzer's equations. Chem. Geol. 39, 165-178.

Guggenheim E. A. (1935) Specific thermodynamic properties of aqueous solutions of strong electrolytes. Phil. Mag. (Series 7) 19, 588-643.

Gustavson T. C., Presley M. W., Handford C. R., Finley R. J., Dutton S. P., Baumgardner R. W. Jr., McGillis K. A. and Simpkins W. W. (1980) Geology and geohydrology of the Palo Duro Basin, Texas Panhandle - a report on the progress of nuclear waste isolation feasibility studies (1979). The Univ. Texas at Austin, Bureau of Econ. Geol. Geologic Circular 80-7, 99 p.

Hardie L. A. (1967) Gypsum-Anhydrite equilibrium at 1 atmosphere pressure. Am. Min. 52, 170-200.

Harned H. S. and Owen B. B. (1958) The Physical Chemistry of Electrolytic Solutions, 3rd Ed. ACS Monograph No. 137.

Harvie C. E. and Weare J. H. (1980) The prediction of mineral solubilities in natural waters: Na-K-Mg-Ca-Cl-SO_4-H_2O system from zero to high concentration at 25°C. Geochim. Cosmochim. Acta 44, 988-997.

Harvie C. E., Eugster H. P. and Weare J. H. (1982) Mineral equilibria in the six-compoinent seawater system, Na-K-Mg-Ca-SO_4-Cl-H_2O at 25°C. II. Compositions of the saturated solutions. Geochim. Cosmochim. Acta 46, 1603-1619.

Harvie C. E. (1981) Theoretical investigations in geochemistry and atom surface scattering. PhD dissertation, Univ. of California, San Diego.

Helgeson H. C. (1981) Theoretical prediction of the thermodynamic behavior of aqueous electrolytes at high pressures and temperatures; IV, Calculation of activity coefficient, osmotic coefficient, and apparent molal and standard and relative partial molal properties to 600°C and 5kb. Am. J. Sci. 281(10) 1249-1516.

Hubbard N. (1984) Personal Communications, ONWI Battelle Memorial Institute, Columbus, OH.

Hurlbut Jr. C. S. and Klein C (1977) Manual of mineralogy, Wiley.

Jenne E. A., Ball, J. W., Burchard J. M., Vivit D. V., and Barks J. H. (1980) Geochemical modelling: Apparent solubility controls on Ba, Zn, Cd, Pb, and F in waters of the Missouri Tri-State mining area: In, Trace Substances in Environmental Health-XIV (D. D. Hemphill, editor) 353-361, University of Missouri, Columbia, MO.

Kreitler C. W., Collins E. W., Fogg G. E., Jackson M. and Seni S. J. (1983) Hydrogeologic characterization of the saline aquifers, East Texas Basin-Implications to nuclear waste storage in East Texas salt domes. DOE Report under Contract DE-AC97-80ET46617.

Kubo H., Bernthal R. and Wildeman T. R. (1978) Energy dispersive X-ray fluorescence spectrometric determination of trace elements in oil samples. Anal. Chem. 50, 899-903.

Kushnir J. (1980) The coprecipitation of strontium, magnesium, sodium, potassium and chloride with gypsum, an experimental study. Geochim. Cosmochim. Acta 44, 1471-1482.

Kushnir J. (1981) The partitioning of seawater cations during the transformation of gypsum to anhydrite. Geochim. Cosmochim. Acta 46, 433-446.

Langmuir D. (1983) Personal communication. Colo. School of Mines.

Langmuir D. (1971) Geochemistry of some carbonate groundwaters in central Pennsylvania. Geochim. Cosmochim. Acta 35, 1023-1045.

Langmuir D. (1978) Uranium solution-mineral equilibria at low temperatures with applications to sedimentary ore deposits, Geochim. Cosmochim. Acta 42, 547-569.

Langmuir D. and Riese A. C. (1984) The thermodynamic properties of some radium dissolved species. Geochim. Cosmochim. Acta (in review).

Latimer W. M. (1952) Oxidation Potentials. Prentice-Hall.

Laul J. C., Perkins R. W. and Hubbard N. (1983) The behavior of natural radionuclides in briney groundwaters. Abstract, 96th Annual meeting Geological Society of America, Indianapolis, IN.

MacDonald R. W. and North N. A. (1974) The effect of pressure on the solubility of $CaCO_3$, CaF_2, and $SrSO_4$ in water. Can. J. Chem. 52, 3181-3186.

Majima H., Awakura Y., Yazaki T. and Chikamori Y. (1980) Acid dissolution of cupric oxide. Metal. Trans. B 11B, 209-214.

Mason B. and Moore C. B. (1982) Principles of Geochemistry 4th Ed. Wiley.

McDowell L. A. and Johnston H. L. (1936) The solubility of cupric oxide in alkali and the second dissociation constant of cupric acid. The analysis of very small amounts of copper. J. Am. Chem. Soc. 5, 2009-2014.

Melchior D. C., Langmuir D., and Rogers P. S. Z. (1984) The thermodynamics and geochemistry of Ca, Sr, Ba, and Ra in brines from the Wolfcamp and Granite Wash Facies, Palo Duro Basin,Texas, with applications to high level nuclear waste disposal. In Preparation.

Meyer S. L. (1975) Data analysis for scientists and engineers. Wiley.

Midgley D. and Torrance K. (1978) Potentiometeric Water Analysis. Wiley.

Millero F. (1983) The estimation of the pK^*_{HA} of acids in seawater using the Pitzer equations. Geochim. Cosmochim. Acta 47, 2121-2131.

Moody J. R. and Lindstrom R. M. (1977) Selection and cleaning of plastic containers for storage of trace element samples. Anal. Chem. 49(14), 2264-2267.

Murray R. C. and Cobble J. W. (1980) Chemical equilibrium in aqueous systems at high temperatures. Proc. The Int. Water Conf. 41st Annual meeting, Pittsburg, Pennsylvania.

Olofsson G. and Olofsson I. (1978) Empirical equations for some thermodynamics quantities for the ionization of water as a function of temperature. J. Chem. Thermo. 13(5), 437-440.

Parkhurst D. L., Thorstenson D. C., and Plummer L. H. (1980) PHREEQE-A Computer program for geochemical calculations. USGS Water-Resources Investigations 80-96.

Pitzer K. S. and Brewer L. (1961) Thermodynamics. McGraw-Hill.

Pitzer K. S. (1973a) Thermodynamics of electrolytes, I. Theoretical basis and general equations. J. Phys. Chem. 77, 268-277.

Pitzer K. S. and Mayorga G. (1973b) Thermodynamics of electrolytes, II. Activity and osmotic coefficients for strong electroytes with one or both ions univalent. J. Phys. Chem. 77, 2300-2308.

Pitzer K. S. and Mayorga G. (1974a) Thermodynamics of electrolytes, III. Activity and osmotic coefficients for 2-2 electrolytes. J. Solution Chem. 3, 539-546.

Pitzer K. S. and Kim J. (1974b) Thermodynamics of electrolytes, IV. Activity and osmotic coefficients for mixed electrolytes. J. Am. Chem. Soc. 96, 5701-5707.

Pitzer K.S. (1975) Thermodynamics of electrolytes. V. Effects of higher order electrostatic terms. J. Solution Chem. 4, 249-265.

Pitzer K. S. (1979) Theory: Ion interaction approach. In: R. M. Pytkowicz (editor), Activity coefficients in electrolyte solutions Vol. 1. Chemical Rubber Company Press, 157-209.

Plummer L. N., Jones B. F. and Truesdell A. H. (1976) WATEQF-A FORTRAN IV version of WATEQ, a computer program for calculating chemical equilibrium of natural waters. USGS Water Res. Inv. 76-13.

Reardon E. (1983) Personal Communication, University of Waterloo.

Robertson D. E. (1968) Role of contamination in trace element analysis of sea water. Anal. Chem. 40(7), 1067-1072.

Robie R. A., Hemingway B. S. and Fisher J. R. (1978) Thermodynamics of minerals and related substances at 298.15K and 1 Bar Pressure and at higher temperatures. USGS Bulletin 1452.

Robinson R. A. and Stokes R. H. (1959) Electrolyte Solutions (2nd Ed.), Academic Press.

Rogers P. S. Z. (1981) Thermodynamics of Geothermal Fluids. Ph.D. dissertation, U. Calif. Berkeley.

Scatchard G. (1936) Concentrated solutions of strong electrolytes. Chem. Rev. 19, 309-327.

Schindler P. W. (1968) Heterogeneous equilibria involving oxides, hydroxides, carbonates, and hydroxide carbonates, In: Equilibria Concepts in Natural Water Systems, W. Stumm, Ed., Advances in Chemistry Series No. 67, American Chemical Society, 196-221.

Skoog D. A. and West D. M. (1974) Analytical Chemistry, an Introduction. Holt, Rinehart, and Winston.

Strübel G. (1966) Die hydrothermole Loslichkeit von Colestin in System $SrSO_4$-NaCl-H_2O. N. Jahrbuch f. Mineralogic, 99-108.

Subramanian K. S., Chakrabarti C. L., Suerias J. E. and Maines I. S. (1978) Preservation of some trace metals in samples of natural waters. Anal. Chem. 50(3), 444-448.

Truitt R. E. and Weber J. H. (1979) Trace metal ion filtration losses at pH 5 and 7. Anal. Chem. 51(2), 2057-2059.

APPENDIX A: DETAILED MODELING EQUATIONS

The general equation and parameter symbols used to obtain the mean activity coefficient of a salt is given in the body of the text.

The mean activity coefficient for $Cu(OH)_2$ in a NaOH solution is:

$$\ln \gamma^{\pm} = 2f^{\gamma} + B_{CuOH}(0.333m_{OH} + 1.333m_{Cu}) + C_{CuOH}(0.666m^2_{OH} + 2.666m^2_{Cu} + 1.333m_{Cu}m_{Na} + 1.333m_{Cu}m_{OH}) + B_{NaOH}(m_{Na}) + C_{NaOH}(2m_{Cu}m_{Na} + m^2_{Na} + 1.333m_{Na}m_{OH}) + \theta_{CuNa}(0.500m_{Na} + m_{Cu}m_{Na}) + \psi_{CuNaOH}(0.333\ m_{Na}m_{OH} + 0.333m_{Cu}m_{Na})$$

However, since B_{NaOH}, C_{NaOH}, and θ_{CuNa} are known, it can be shown:

$$\ln \gamma^{\pm} = \ln \gamma^{*} + B_{CuOH}\ (0.666m_{OH} + 1.333m_{Cu}) + C_{CuOH}\ (0.666m^2_{OH} + 2.666m^2_{Cu} + 1.333m_{Cu}m_{Na} + 1.333m_{Cu}m_{OH}) + \psi_{CuNaOH}(1.333m_{Na}m_{OH} + 1.333m_{Cu}m_{Na})$$

where $\ln \gamma^{*}$ is a summation of known terms.

If NaCl is added to the NaOH solution, the unknown in the resulting equation are identical to those needed to describe dissolution of CuO in $CuCl_2$ solutions and is:

$$\ln \gamma^{\pm} = \ln \gamma^{*} + B_{CuOH}\,(0.666m_{OH} + 2m_{Cu}m_{Cl} + 1.333m_{Cu}) + C_{CuOH}(0.666m^{2}_{OH} + 2.666m^{2}_{Cu} + 1.333m_{Cu}m_{OH} + 0.666m_{OH}m_{Cl}) + \psi_{CuOHCl}(0.666m_{Cu}m_{OH} + 0.666m_{Cu}m_{Cl} + 0.166m_{OH}m_{Cl})$$

The same relationships exist for dissolution of tenorite in Na_2SO_4 solutions yielding the equation:

$$\ln \gamma^{\pm} = \ln \gamma^{*} + B_{CuOH}\,(0.666m_{OH} + 1.333m_{Cu} + 2m_{Cu} + 2m_{Cu}m_{SO_4}) + C_{CuOH}(0.666m^{2}_{OH} + 1.333m_{OH}m_{SO_4} + 2.666m^{2}_{Cu} + 1.333m_{Cu}m_{Na} + 1.333m_{Cu}m_{OH}) + \psi_{CuOHSO_4}(0.666m_{Cu}m_{SO_4} + 0.666m_{Na}m_{SO_4} + 0.333m_{OH}m_{SO_4})$$

Thus, the γ's may be obtained by several differing approaches.